

PROGRESSIVE DAMAGE MODELING OF PIN LOADED COMPOSITE PLATE USING FEMA

A Thesis submitted
in partial fulfillment of the requirements for
the award of degree of
MASTER OF ENGINEERING
IN
CAD/CAM & ROBOTICS ENGINEERING

Submitted By
BIKRAMJIT SHARMA

Roll No. 8048105
Under the supervision of

Dr. V.K. Jadon

Mr. K.Khanna



MECHANICAL ENGINEERING DEPARTMENT
THAPAR INSTITUTE OF ENGINEERING AND TECHNOLOGY
(Deemed University)
PATIALA-147004, (INDIA)

2006

CERTIFICATE

This is to certify that the Thesis titled, “**Progressive Damage Modeling Of Pin Loaded Composite Plate Using FEMA**”, submitted by **Mr. Bikramjit Sharma**, in partial fulfillment of the requirements for the award of degree of **Master of Engineering (CAD/CAM & Robotics Engineering)** at **Thapar Institute of Engineering and Technology (Deemed University), Patiala** is a bonafide work carried out by him under my guidance and supervision and that no part of this thesis has been submitted for the award of any other degree.

(Dr. Vijay Kumar Jadon)

Assistant Professor, MED

T.I.E.T., Patiala-147004

(Mr. Kishore Khanna)

MED, T.I.E.T., Patiala

Countersigned By:

(Dr. S.K. MOHAPATRA)

Prof. and Head, MED

T.I.E.T., Patiala-147004

(Dr. T.P. Singh)

Dean of Academic Affairs

T.I.E.T., Patiala-147004

ACKNOWLEDGEMENT

I express my sincere gratitude to my guide, **Dr. Vijay Kumar Jadon**, Asst. Professor, Mechanical Engineering Department, Thapar Institute of Engineering and Technology, Patiala, for his valuable guidance, proper advice, painstaking and constant encouragement during the course of my work on this thesis.

I am also thankful to **Mr. Kishore Khanna**, Mechanical Engineering Department, Thapar Institute of Engineering and Technology, Patiala who devoted his valuable time and helped me in all possible ways towards successful completion of Thesis. I do not find enough words with which I can express my feeling of thanks to entire faculty and staff of M.E.D., T.I.E.T., Patiala, for their help, inspiration and moral support which went a long way in successful completion of my thesis. I thank all those who have contributed directly or indirectly to my thesis.

(Bikramjit Sharma)

NOMENCLATURE

[B]	Strain displacement matrix
$\{d^i\}$	Global nodal displacement vector
$\{\dot{d}\}$	Velocity vector
$\{\ddot{d}\}$	Acceleration vector
[D]	Elasticity Matrix
E	Young's Modulus of elasticity
F_τ	Surface Traction force
F_B	Body force
$\{F_{\epsilon_0}\}^e$	Elemental nodal initial strain vector
$\{F_{\sigma_0}\}^e$	Elemental nodal residual stress vector
$\{F_\tau\}^e$	Elemental nodal surface traction vector
$\{F_{BS}\}^e$	Elemental nodal static body force vector
G	Shear Modulus
[K]	Stiffness matrix
[M]	Mass matrix
$[\tilde{N}]$	Displacement Shape function matrix
u, v, w	Displacement field in X, Y, Z directions
x, y, z	Cartesian operator
δ	Variational operator
ρ	Mass density
ϵ	Strain field
σ	Stress field
ϵ_0	Initial strain vector
σ_0	Residual stress vector
u	Poisson's ratio
π_p	Potential energy function
T	Transpose of matrix or vector
e	Element matrix or vector

INDEX

CONTENTS.	PAGE NO.
List of Figures	iii
List of Tables	iv
Abstract	v
1 INTRODUCTION	1-6
1.1 Introduction	
1.2 Composite Materials	
1.3 Classification of Composite Materials	
1.3.1 Based on Reinforcement Geometry	
1.3.2 Based on Matrix	
1.4 Present Work	
2 REVIEW OF LITERATURE	7-14
3 ANALYSIS	15-28
3.1 Introduction	
3.2 Theorem of Minimum Potential Energy	
3.3 Finite Element Analysis of 2-D Quadrilateral elements	
3.4 Concept of Composite Lamina	
3.5 Lamina Subjected to in-plane loading	
3.6 Damage Analysis	
4 SOLUTION SCHEME	29-34
4.1 Equation Solution Scheme	
4.2 Computational Procedures	
4.2.1 Damage Analysis	
4.3 Program Structure	
5 RESULTS AND DISCUSSIONS	35-44
5.1 Introduction to Problem	
5.2 Finite Element Meshing	

- 5.3 Boundary Conditions
- 5.4 Validation of work
- 5.5 Failure strength of laminates with different lay-ups.
- 5.6 Discussions

6 CONCLUSION AND FUTURE SCOPE 45

- 6.1 Conclusion
- 6.2 Scope for future work

REFERENCES

LIST OF FIGURES

Figure No.	TITLE	PAGE No.
1.1	Classification of Composite Materials	3
1.2	Morphology of Reinforcement in Matrix	4
3.1	Composite Lamina Structure	22
3.2	Local and Global Coordinate System	23
3.3	Transformation of Local coordinate System to Global Coordinate System	25
3.4	Composite Material Stack	26
4.1	Flow Chart for the Main Program	31
4.2	Flow chart for Calculating Elemental Stiffness Matrix	33
4.3	Flow chart for Calculation of Jacobian Matrix	34
5.1	Specimen Configuration	35
5.2	Finite Element Discretization of the Specimen	37
5.3	Boundary Conditions and Forces Applied to the Specimen In Finite Element Model.	38
5.4	Problem Taken for Validation	39
5.5	Illustration of Damage Propagation at Different Load Steps	40
5.6	Illustration of Damage Propagation for (E/D=4;W/D=4; $\theta=0$)	40
5.7	Illustration of Damage Propagation for (E/D=4;W/D=4; $\theta=15,30,45$)	40
5.8	Comparison of Results (Hoffman Failure Criteria)	41
5.9	Comparison of Results (Hashin's Failure Criteria)	42
5.10	Laminate Scheme	42
5.11	First Failure Load for $[0\pm45]_s, [90\pm45]_s,$ $[0/90/0/90/0/90]$ Lay-Ups	43
5.12	Final Failure Load for $[0\pm45]_s, [90\pm45]_s,$ $[0/90/0/90/0/90]$ Lay-Ups	44

LIST OF TABLES

TABLE No.	TITLE	PAGE No.
5.1	Specimen Dimensions	35
5.2	Elastic Material constants (tensile and compressive)	36
5.3	Material parameters for Damage Analysis(in MPa)	36
5.4	Comparison of Results	41
5.5	Material Parameters for Damage Analysis of Laminate	43
5.6	First failure Load for Different Lay-Ups	43
5.7	Final Failure Loads	43

ABSTRACT

The aim of this study is to determine the progressive damage in composite plate using finite element methods. The current model is two-dimensional progressive damage model consisting of four noded quadrilateral elements. The methodology for modeling the joint problem which consists of three steps: stress analysis, application of failure analysis and property degradation rules is utilized into a working model. To determine the failure of laminate during progressive application of static load Hashin's failure criteria and Hoffman's Failure criteria have been used. Once a ply fails the material properties have been degraded using associated degradation rules.

A computer programme developed for such an analysis is used to calculate the failure load, the failure mode, and the propagation of failure of plate with different fiber orientation and different geometries.

CHAPTER 1

INTRODUCTION

1.1 INTRODUCTION

The quest for increased performance and efficiency in the aerospace industry has resulted in the need to utilize composite materials in a greater percentage of structural components. The high strength to weight and stiffness to weight characteristics of fiber reinforced, polymer matrix composites (P.M.C's) has made them desirable for use in aerospace applications, where weight savings are crucial .

In order to join the several parts of such structures, bolted or riveted joints are often selected, due to the fact that these joints are easy to assemble, to allow component disassembly and repair or substitution, and are tolerant to environmental effects. However, mechanically fastened joints due to stress concentration created are a source of weakness and contribute to an excess of weight. The joints are very often a critical part of a structure. The soundness of their design procedures on the overall weight and cost of the product need to be considered. Therefore, reliable and general joint design methods in composite structures are required to avoid unnecessary weight and both product and in-service cost penalties. To utilize the full potential of composite materials as structural elements, the strength and failure of mechanically fastened joints in composite plates must be understood.

The objective of this study is to develop a model capable of predicting the response of laminated composite material subjected to static bolt bearing loads. Specifically, the localized time-dependent deformations and damage accumulation in the vicinity of loaded holes are of primary concern. The developed finite element code can be used for a variety of laminates, component geometries, loading conditions etc.

1.2 COMPOSITE MATERIALS

A composite material is a mixture of two or more distinct constituents or phases. But this definition is not sufficient and three other criteria have to be satisfied before the material can be said to be a composite. First, both constituents have to be in reasonable proportions, say greater than 5%. Secondly, it is only when the constituents phases having different properties, and hence the composite properties are noticeably different from the properties of the constituents. Thirdly, there are distinct, recognizable interfaces between the constituent phases.

Depending on the properties, relative amounts, degree of bonding & orientation of various constituents along with the size, shape & distribution of discontinuous constituents, composite materials possesses characteristics properties, such as stiffness strength, weight, high temperature performance, corrosion resistance, hardness, which are not possible with the individual constituents.

History of Composites

One of the earliest known composite materials is adobe brick in which straw (a fibrous material) is mixed with mud or clay (an adhesive with strong compressive strength). The straw allows the water in the clay to evaporate and distributes cracks in the clay uniformly, greatly improving the strength of this early building material. Another form of a composite material is the ubiquitous construction material we call plywood. Plywood uses natural materials (thin slabs of wood) held together by a strong adhesive, making the structure stronger than just the wood itself. In nature, bamboo is often cited as an example of a wood composite structure, combining a cellulose fiber and lignin, with the lignin providing the adhesive to hold the fibers together.

Reinforced concrete is a combination of two remarkable materials, concrete (a composite by itself) and steel that takes advantage of the strengths of each material to overcome their individual limitations in each. Steel has very high tensile strength, while concrete has very high compressive strength. In combination, they make a superior material for road and bridge construction.

Today, when we speak of composite materials, or just 'composites', we are referring to the highly engineered combinations of polymer resins and reinforcing materials such as glass fibers. A fiberglass composite structure is a

combination of glass fibers of various lengths and resins such as vinyl ester or polyester. The term FRP is often used, meaning Fiber Reinforced Plastic. FRP is a very general term for many different combinations of reinforcement materials and bonding resins. Thus, the term “composites” is used extremely broadly to describe many materials with many different properties targeted at an even larger number of applications. To show how composites have changed our world, look no further than under the hood of a modern car and realize that most of what we can see is components made of composite materials. If the car is a Corvette, the entire body is made of fiberglass or carbon reinforced composite materials.

1.3 CLASSIFICATION OF COMPOSITE MATERIALS

Composites are classified [20] by the geometry of the reinforcement as particulate, flake and fiber or by the type of matrix as polymer, metal, ceramic and carbon as shown in figure 1.1.

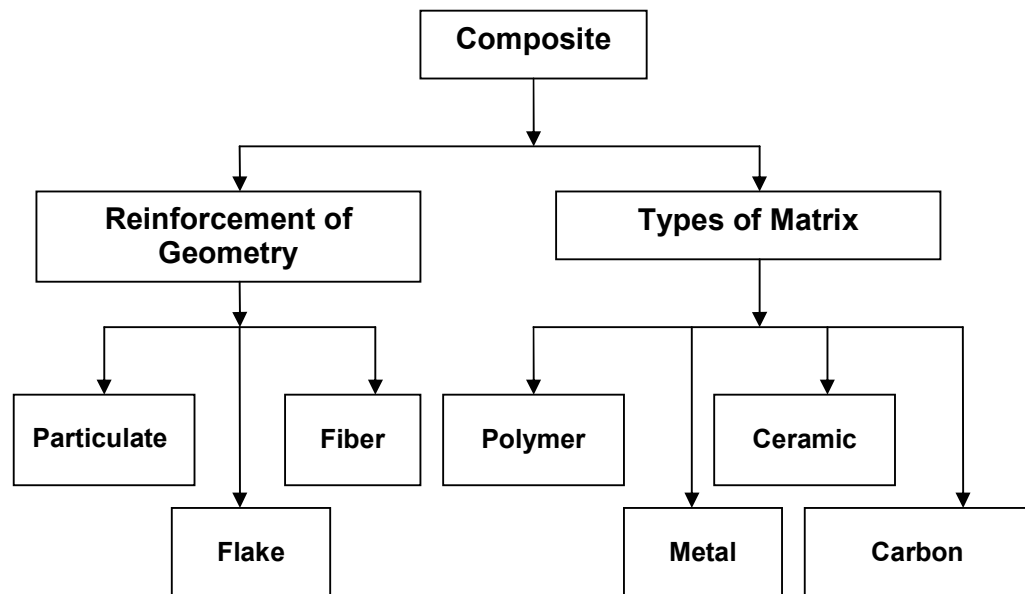


Figure 1.1 Classification of Composite Materials

1.3.1 Based on Reinforcement Geometry

Composites can be classified on the basis of Reinforcement geometry as:

- i. **Particulate Composite**

It consists of particles immersed in matrices such as alloy and ceramics. They are usually isotropic since particles are added randomly. Particulate composite has advantages such as improved strength, increased operating temperature and oxidation resistance etc. Eg:-Use of Aluminum particles in rubber, Silicon particles in aluminum.

ii. Flake composite

It consists of flat reinforcements of matrices. Typical flakes Materials are Glass, Mica, Silica, Silver etc. Flake composites provide advantages such as high out-of-plane flexural modulus, higher strength and low cost. However flakes can not be oriented easily and only a limited number of materials are available for use

iii. Fiber composite

It consist of matrices reinforced by short (discontinuous) or long (Continuous) Fibers. Fibers are generally anisotropic. Examples of matrices are resins such as epoxy, metals such as Aluminum and Ceramics such as Calcium-Alumino Silicate.

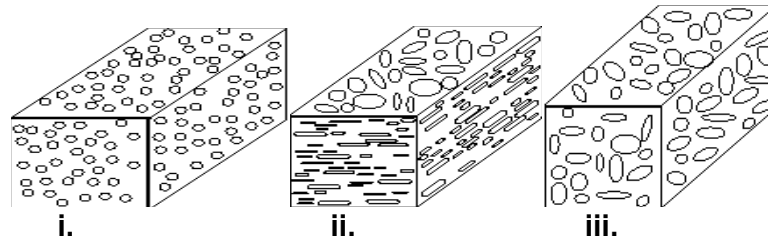


Figure 1.2: Morphology of Reinforcement in Matrix

1.3.2 Based on Matrix

On the basis of Matrix the Composites are classified as:

i. Polymer Matrix Composite

These are most common advanced composites. These composite consist of a polymer (epoxy, polyester, urethane etc) reinforced by thin diameters fibers (graphite, aramids, and boron).Graphite/Epoxy composites are approximately five times stronger than steel on a weight-to-weight basis. They are most common because of their low cost, high

strength and simple manufacturing. Main drawbacks of polymer laminate composite (P.M.C.) include low operating temperature, high coefficient of thermal and moisture expansion and low elastic properties in certain direction. Its advantages include its strength, low cost, high chemical resistance and good insulating property.

ii. Metal Matrix Composite

It has a metal matrix. Examples of matrices are Aluminum, Magnesium and Titanium. Typical fiber includes carbon, silicon carbide. Metals are reinforced to increase or decrease their properties to suit the needs of design. Ex:-The elastic stiffness and strength of metals can be increased, while large coefficients of thermal expansion and thermal and electric conductivities of metal can be reduced by addition of fiber such as silicon carbide.

iii. Ceramic Matrix Composite

Ceramic matrix composites (C.M.C.) have a ceramic matrix such as alumina, calcium, aluminosilicate reinforced by fibers such as carbon or silicon carbide. Advantages:- high strength, hardness, high service temperature limit for ceramics, chemical inertness and low density. Area of application: - C.M.C. are finding increased application in high temperature areas where M.M.C's and P.M.C's cannot be used.

iv. Carbon-Carbon Composite

Carbon-carbon composites use carbon fiber in carbon matrix. These composites are used in very high temperature environments of up to 6000⁰F (3315⁰C) and are 20 times stronger and 30% lighter than graphite fibers. Advantages:-ability to withstand high temperatures, low creep at high temperature, low density, good tensile and compressive strength, high fatigue resistance, high thermal conductivity and high coefficient of friction. Disadvantages:-high cost, low shear strength and susceptibility to oxidations at high temperature. Area of application:- space shuttle nose cone, aircraft brakes, mechanical fasteners etc.

v. Aluminium / Aluminium Alloy Based Metal Matrix Composite

In research and development as well as in various industrial applications, MMC's based on Aluminium and its alloy are widely used. This is because Aluminium is light in weight which is the primary requirement in

most of the applications of the metal matrix composite. Additionally, it is economical in comparison with other light metals, such as titanium and magnesium. Further its excellent strength, ductility and corrosion properties are well established and they can be modified to fulfill the requirement of many different applications ranging from automotive and aircraft industry to sports and leisure.

Polymer composites are the most advanced composites. These composites consist of a polymer (e.g., epoxy, polyester, urethane) reinforced by thin-diameter fibers (e.g., graphite , aramids, boron).These are commonly employed due to their low cost, high strength, and simple manufacturing principle. As an example, graphite /epoxy composites are approximately five times stronger than steel on a weight-for-weight basis.

1.4 PRESENT WORK

In the present work, 2D finite element model have been developed for damage analysis of statically loaded composite plate. The well known variational theorem of minimum potential energy has been modified for a laminate subjected to in-plane loading only (no bending moments).A set of ply failure criteria, and a property degradation model has been used. The developed finite element code has been used to calculate the failure load, the failure mode, and the propagation of failure of plates with different fiber orientation, different edge distances, and different width to diameter ratios.

CHAPTER 2

REVIEW OF LITERATURE

Various analytical and numerical approaches have been developed for the analysis of composite structural joints. Some of the work related to present study is illustrated in the following paragraphs.

Fu-Kuo Chang et.al. [1] presented a progressive damage model for notched laminated composites subjected to tensile loading. The model was capable of assessing damage in laminates with arbitrary ply-orientations and of predicting the ultimate tensile strength of the notched laminates. The model consists of two parts, namely, the stress analysis and failure analysis. Stresses and strains in laminates were analyzed on the basis of classical lamination theory with the consideration of material non-linearity. Damage accumulation in laminates was evaluated by proposed failure criteria combined with a property degradation model

H.J.Lin et.al. [2] investigated the failure strength and failure mode of bolted connections of glass woven fabric composites. For investigation purpose Circular holes of two types, drilled and moulded-in, were considered. An incremental two-dimensional finite element code, based on the Hashin strength criterion and a progressive damage model, was used in the analysis of damage propagation and ultimate joint strength of laminates. The failure criteria and the material degradation model were successfully used to model the behavior of laminates subjected to in-plane loads. They considered five types of failures: matrix failure in tension, matrix failure in compression, fiber failure in tension, fiber failure in compression and fiber-matrix debonding failure. Failures of these type resulted in local degradation of material. The area in which failure was detected, material properties were thus degraded according to the material degradation model. Thus In the failure analysis, the stress distribution of laminates with drilled and moulded-in holes was analyzed by the finite element method. The failure mode and failure strength of $[0/90]$, and $[\pm 45]_s$, laminates with various hole diameters and values of E/D were analyzed. Experimental results showed that laminates with moulded-in holes are stronger when the

edge distance is small. When the edge distance was large, specimens with moulded-in holes have about the same strength as those with drilled holes.

Nahla K. Hassan et.al. [3] conducted a three-dimensional finite element analysis using the ANSYS program to perform stress analysis of single and multi bolted double shear lap connections of glass fiber reinforced plastic, taking into consideration the bolt hole contact problem. In this study the three-dimensional shell element was used and element displacement fields were calculated. After that the Hooke's law relating the stresses and strains for transversely isotropic material was used. The stress components, obtained by the finite element analysis were used to predict the maximum allowable stress in the laminate through the use of the failure criterion.

Xiong et.al. [4] proposed modeling procedures for stress analysis of riveted lap joints in aircraft structure, using both analytical and numerical methods. In the analytical method, a complex variational approach was employed to determine the stresses in joined plates containing single or multiple loaded holes. The effects of finite geometry were taken into account by the variational formulations. An iterative scheme was carried out to handle the deformation compatibility between all joined members. In the numerical method, finite element analysis was conducted. A major difficulty in modeling riveted joints was the idealization of the load transfer between the rivet and the plate. Therefore several alternative strategies for FE modeling were investigated in the programme on multiple site damage in lap joints. For comparison with analytical method, the two-dimensional modeling method using the commercial packages were used.

Camanho et.al. [5] developed a three-dimensional finite element model to predict damage progression and strength of mechanically fastened joints in carbon fiber-reinforced plastics that fail in the bearing, tension and shear-out modes. The model was based on: a three-dimensional finite element model, a three-dimensional failure criterion and a constitutive equation that takes into account the effects of damage on the material elastic properties. This was accomplished using internal state variables that were functions of the type of damage. This formulation was used together with a global failure criterion to predict the ultimate strength of the joint. Experimental results concerning damage progression, joint stiffness and strength were obtained and compared

with the predictions. A good agreement between experimental results and numerical predictions was obtained.

Aktas et.al. [6] investigated failure strength and failure mode of a mechanically fastened carbon-epoxy composite plate of arbitrary orientation. The plate was considered as symmetric and hence only half of plate was modeled. First, the stress distribution in the plate was calculated by the use of finite-element method. Second, the failure load and the failure mode were predicted by means of Tsai-Hill and fiber tensile-compressive failure criteria. A computer program was developed which can be used to calculate the failure load, the failure mode, and the propagation of failure through the plate. Bearing strength and failure modes were taken as functions of three variables: orientation angle of fibers, E/D , and W/D . By changing the value of one of the variables while keeping the values of the others constant, experimental and numerical analyses were performed.

Kermenidis et.al. [7] developed a three-dimensional progressive damage model to simulate the damage accumulation of bolted single-lap composite joints under in-plane tensile loading. The model was capable of predicting the residual strength and residual stiffness of laminates with arbitrary lay-ups, geometries and bolt positions. The parametric study included stress analysis, failure analysis and material property degradation. Stress analysis of the three-dimensional geometry was performed using the ANSYS FE code. Failure analysis and degradation of material properties were implemented using a progressive damage model, which was incorporated in ANSYS macro-routine. The progressive model utilized a set of stress-based Hashin's criteria and a set of appropriate degradation rules. A parametric study was performed to examine the effect of bolt position and friction upon residual strength and damage accumulation.

Dano et.al. [8] carried out analysis on single mechanically fastened joint in fiber-reinforced plastics. A finite-element model was developed to predict the response of pin-loaded composite plates. The model takes into account contact at the pin-hole interface, progressive damage, large deformation theory, and a non-linear shear stress-strain relationship. To predict the progressive ply failure, the analysis combined Hashin and the maximum stress failure criteria. The objective of the study was to determine the influence of the failure criteria and

the inclusion of a non-linear shear behavior on the strength prediction and the load-pin displacement curve. The proposed model was used to predict the bearing response of composite plates with different stacking sequences. Good agreement between experimental results and numerical predictions was observed.

Li et.al. [9] described the tensile response and failure of composite riveted joints. They tested 7-joint configuration for aircraft application at quasi-static, 4 and 8 m/s nominal loading rates. Joint specimens were made of CFRP in a number of lay-ups of unidirectional tapes and woven fabrics. A dynamic tensile test method was designed to give reliable test- results. It was shown that the variation of tensile strength with loading rate was negligible for the tested composite riveted joints. However, for the most of the tested specimens, the average total energy absorption of the composite joint increased with increasing load rate. Various failure modes were identified for various joint designs and it was found that joint failure modes can change with varying load rates.

Okoli et.al. [10] performed tensile test according to method prescribed in ASTM D 3039. The laminates were glass/epoxy, 3mm thick composite sheets. The glass was a cross-ply plain weave [0/90] fabric. The composite had a fiber weight fraction of 70% with 18 layers of glass. The specimens were cut in dimensions of 200mm x 15 mm. Aluminium tabs 1 mm thick and 50 mm long were locally bounded to the specimens with an adhesive, leaving a gauge section of 100 mm. Strain gauges were bounded on either side of the specimen with adhesive, to measure the axial and transfer strain on the material during testing. All data were logged to a personal computer via a data logger. The low rate tensile tests were performed on a screw driven tensile testing machine at four different cross head velocities. Further tests were carried out at a high rate on a hydraulic tensile testing at four cross head velocities. The test force was measured with a piezo quartz load cell.

It was demonstrated that a tensile modulus of elasticity and tensile strength of glass fibers increases with strain rate. It was also observed that the energy involved in the failure of FRC specimens as determined from the area under the stress-strain curve, increases with strain rate.

Tserpes et.al. [11] conducted a parametric finite element analysis to investigate the effect of failure criteria and material property degradation rules

on the tensile behavior and strength of bolted joints in graphite/epoxy composite laminates. The analysis was based on a three-dimensional progressive damage model (PDM) developed earlier by the authors. The PDM comprises: the components of stress analysis, failure analysis and material property degradation. The predicted load–displacement curves and failure loads of a single-lap single-bolt joint were compared with experimental data for different joint geometries and laminate stacking sequences. The stiffness of the joint was predicted with satisfactory accuracy for all configurations. The predicted failure load was significantly influenced by the combination of failure criteria and degradation rules used. A combination of failure criteria and material property degradation rules that lead to accurate strength prediction was proposed. For all the analysis performed, the macroscopic failure mechanism of the joint and the damage progression were also predicted.

Bulent Murat Icten et.al. [12] Investigated the possibility of predicting the properties of the joint from the properties of the material measured with standard tests. A composite rectangular plate of length $L+E$ and width W with a hole of diameter D , with a hole at a distance E , from the free edge of the plate was taken as the specimen. A rigid pin was located at the center of the hole and a uniform tensile load P was applied to the plate. A compression testing was applied to the specimen to find failure in net-tension, shear out mode, and bearing mode. A progressive damage model was applied which consisted of three: stress analysis, failure criteria, and property degradation rules. The two-dimensional finite element method was used to determine the failure load and failure mode using Hoffman and Hashin criteria. The mechanical properties of the composite material were obtained from standard tests. Load displacement curves for various W/D , the effect of W/D ratio, and orientation on bearing strength were plotted and results were in close agreement with the experimental results.

Okutan et.al. [13] performed an investigation to study the response of pin-loaded laminated composites. Tensile tests were performed on E/glass-epoxy composites for two different ply orientations such as $[0/\pm 45]_s$ and $[90/\pm 45]_s$. For each ply orientation, 20 different geometries were chosen. The major focus of the study was to characterize the failure mechanisms and to evaluate the effect of geometric dimensions on the bearing, shear-out and net-

tension strengths of pinned joints. For this purpose, the specimens were tested to find first failure and final failure load. In addition, by using finite element code PDNLPIN, a static progressive failure analysis was performed. The effect of the material non-linearity was taken into account on the mathematical forms. Comparisons were made between the test data and the results of the model and these showed good agreements.

B. Yang et.al. [14] presented a three-dimensional (3-D) stress analysis model for composite laminates with a pinned circular hole. The effects of friction, bearing force and bypass loading on the stress redistribution were studied in detail and an efficient and accurate numerical method for analyzing the mechanical behavior of a composite laminate plate with an elastically pinned circular hole under a bearing force on the pin loading in the composite was presented. The composite laminates were considered to be generally anisotropic and the pin to be isotropic. The problem was solved by using a novel 3-D boundary element formulation where the fundamental solution employs the Green's function for anisotropic multilayer that satisfy the continuity conditions of displacement and traction across the interfaces and the traction-free and symmetry conditions on the top and bottom surfaces. It had been shown that the presence of friction in the joint reduces the magnitude of contact pressure but induces non-trivial shear traction. The distribution of other stress components is also altered. It also leads to the complicated loading-history dependence of stress state, such as dependence on loading sequence of applying the bearing force and bypass loading, and on load cycling.

J. Wang et.al. [15] tested quasi-isotropic AS4/3501-6 laminate coupons in tension and compression. The Basic lamina properties were determined experimentally and then Numerical analyses using linear elastic and progressive damage approaches were conducted. The linear elastic model either significantly underestimated (first-ply failure approach) or overestimated (last-ply failure approach) the strength of un-notched laminates. The progressive damage approach was able to predict accurately the un-notched strength, providing that the non-linear shear behavior was accounted for and appropriate failure criteria used. It was also demonstrated that the progressive damage approach could be implemented, with satisfactory accuracy and efficiency, for open-hole strength prediction using basic material degradation

laws, a shell element model and widely available commercial FEM software (ABAQUS). ABAQUS, a commercial FEM software package was used to predict the strength of un-notched and notched laminates. The progressive failure behavior was simulated by incorporating basic ply failure criteria and degraded material properties.

E.J. Barbero et.al. [16] presented a new model for damage evolution in polymer matrix composites which accounts for different initiation, evolution and failure of two main constituents (fiber and matrix). The material parameters were determined by modeling standard material tests and adjusting individual material parameters to reproduce the observed material response. The overall damage model was based on the combination of damage models for fiber, matrix, and interphase. All three damage models were based on the concepts of continuous damage mechanics.

C.T. McCarthy et.al. [17] presented 3D progressive damage finite element model of multi-bolt, double-lap composite joints developed in the non-linear finite element code ABAQUS. The joint under investigation was of double-lap configuration and consisted of three bolts 'in-line', six washers, three nuts, two splice plates (outer plates) and one skin plate (middle plate). The laminate was modeled using ABAQUS and then a well-known failure theory Hashin failure criteria was implemented in code to determine the mode of failure. Validation was performed by comparing joint load–displacement characteristics and strains with experimental values. The model was then shown to predict joint load distributions that were in close agreement with experimental values. The progression of damage in the joint with increasing load was also presented.

Tayfun Gulem et.al. [18] carried out a study to deal with the bearing strength, failure mode and failure load in a woven laminated glass–vinylester composite plate with circular hole subjected to a traction force by a rigid pin. They investigated for two variables; the distance from the free edge of the plate-to-the diameter of the hole (E/D) ratio and the width of rectangular plate-to-the diameter of the hole (W/D) ratio numerically and experimentally. The numerical study was performed by using 3D FEM with assistance of LUSAS 13.4 finite element analysis program. Hashin failure criteria was used in the failure analysis. The woven glass–vinyl ester composite material was produced and the mechanical properties of the composite material obtained from standard

tests. Experimental results concerning damage progression and ultimate strength of the joint were obtained and compared with predictions. A good agreement was obtained between experimental results and numerical predictions.

With the above study it has been seen that a progressive damage analysis consists of three important steps: stress analysis, application of failure criteria and degradation of material properties according to failure mode. All this is explained in detail in next chapter.

CHAPTER 3

ANALYSIS

3.1 INTRODUCTION

The finite element method is a technique in which a given domain is represented as collection of simple elements, so that it is possible to systematically construct the approximate functions needed in a variational or weighted residual approximation of the solution over each element.

In present study the well known variational principle "The theorem of minimum potential energy" in theory of elasticity is used to solve the problem with help of finite element method.

The theorem of minimum potential energy presents a general formulation for stress analysis of any problem. It is possible to solve the governing equation for complex systems in a very effective way. Numerical solution of the problem discussed is presented in Finite Element Method formulated by using minimum potential energy theorem. This formulation is modified for composite structures by using stiffness matrix for composites. The properties of material are to be degraded in the failed ply by implementing the sudden degradation rule. The scope of using degradation rules is to disable the point from carrying a certain load. When stress in any element dose not obeys the failure criteria, then degrading of the material properties is done and further analysis continued till lamina totally fails.

3.2 THEORM OF MINIMUM POTENTIAL ENERGY

For an elastic continuum problem, the total potential energy is defined as:

$$\Pi_p = U_s - W_e \quad \dots\dots\dots (3.1)$$

Where

$$U_s = \frac{1}{2} \int \epsilon^T \sigma \cdot dv \quad \dots\dots\dots (3.1a)$$

=strain energy of the system, and

$$W_e = u^T F \Big|_r \quad \dots\dots\dots (3.1b)$$

= Potential energy due to external loads

For minimum value of potential energy, the variation of \prod_p should be zero.

Hence

$$\delta\pi_p = \delta(U_s - W_e) = 0 \quad \dots\dots\dots(3.2)$$

For three dimensional stress field, the expression for potential energy due to external loads and strain energy can be written as:

$$\begin{aligned} \delta W_e = & \iint (\delta u.F_{\tau_x} + \delta v.F_{\tau_y} + \delta w.F_{\tau_z})d\tau \\ & + \iiint (\delta u.F_{xb} + \delta v.F_{yb} + \delta w.F_{zb})dv \quad \dots\dots\dots(3.3) \end{aligned}$$

Where,

$F_{\tau_x}, F_{\tau_y}, F_{\tau_z}$ are components of surface tractions per unit area and F_{xb}, F_{yb}, F_{zb} are body force components per unit volume in x,y and z direction respectively.

And

$$\begin{aligned} \delta U_s = & \iiint (\delta\varepsilon_x.\sigma_x + \delta\varepsilon_y.\sigma_y + \delta\varepsilon_z.\sigma_z \\ & + \delta\gamma_{xy}.\tau_{xy} + \delta\gamma_{yz}.\tau_{yz} + \delta\gamma_{xz}.\tau_{xz})dv \quad \dots\dots\dots(3.4) \end{aligned}$$

Where

$$dv = dx.dy.dz \quad \dots\dots\dots(3.5)$$

And $\delta\varepsilon_x, \delta\varepsilon_y, \delta\varepsilon_z, \delta\gamma_{xy}, \delta\gamma_{yz}, \delta\gamma_{xz}$ are virtual strain components.

On substituting Eqns (3.3) and (3.4) in Eqn (3.2) we get

$$\begin{aligned} \delta\prod_p = & \iiint (\delta\varepsilon_x.\sigma_x + \delta\varepsilon_y.\sigma_y + \delta\varepsilon_z.\sigma_z + \delta\gamma_{yz}.\tau_{yz} + \delta\gamma_{xy}.\tau_{xy} + \delta\gamma_{xz}.\tau_{xz})dv - \\ & \iint (\delta u.F_{\tau_x} + \delta v.F_{\tau_y} + \delta w.F_{\tau_z})d\tau - \iiint (\delta u.F_{xb} + \delta v.F_{yb} + \delta w.F_{zb})dv = 0 \quad \dots\dots (3.6) \end{aligned}$$

Introducing following matrix notations:

$$\begin{aligned} u^T &= [u \quad v \quad w] \\ \delta u^T &= [\delta u \quad \delta v \quad \delta w] \\ F_{\tau}^T &= [F_{\tau_x} \quad F_{\tau_y} \quad F_{\tau_z}] \\ F_B^T &= [F_{xb} \quad F_{yb} \quad F_{zb}] \end{aligned}$$

Using above matrix notations Eqn (3.6) is given by

$$\delta\pi_p = \sum_{e=1}^{ne} \delta\pi_p^{(e)}$$

$$= \sum_{e=1}^{ne} (\iiint \delta \varepsilon^T \sigma dv_e - \iint \delta u^T F_\tau d\tau_e - \iiint \delta u^T F_B dv_e) \dots\dots\dots (3.7)$$

$$= 0$$

where ne is number of elements in discretized solution domain.

(i) Displacement Function

$$d = \text{displacement function} = \{d(x,y)\} = \begin{Bmatrix} u \\ v \\ w \end{Bmatrix}$$

thus

$$d = u = \bar{N}d^e \text{ or } \delta u = \bar{N}\delta d^e \dots\dots\dots (3.8)$$

and

$$u^T = d^{eT} \bar{N}^T \text{ or } \delta u^T = \delta d^{eT} \bar{N}^T \dots\dots\dots (3.8a)$$

Where N is shape function matrix

(ii) Strain Displacement Relations

$$\varepsilon = Bd^e \dots\dots\dots (3.9)$$

So,

$$\delta \varepsilon = B\delta d^e \text{ or } \delta \varepsilon^T = \delta d^{eT} B^T \dots\dots\dots (3.9 a)$$

(iii) Stress-strain Relations

$$\sigma = D(\varepsilon - \varepsilon_0) + \sigma_0 \dots\dots\dots(3.10)$$

Where

$$\varepsilon_0 = \{\varepsilon_0\} = \{\varepsilon_{x0} \quad \varepsilon_{y0} \quad \varepsilon_{z0} \quad \gamma_{xy0} \quad \gamma_{yz0} \quad \gamma_{zx0}\}^T$$

=initial strain due to thermal change, shrinkage etc.

$$\sigma_0 = \{\sigma_0\} = \{\sigma_{x0} \quad \sigma_{y0} \quad \sigma_{z0} \quad \tau_{xy0} \quad \tau_{yz0} \quad \tau_{zx0}\}^T \text{ and}$$

$D=[D]$ =Elasticity matrix

(iv) Inertia force

Let $\{u, v, w\}$ = Acceleration vector = $\begin{Bmatrix} u \\ v \\ w \end{Bmatrix}$

ρ = density

Inertia force per unit volume = $-\rho \ddot{u}$

Static body force per unit volume = FBS

Thus

$$F_B = (F_{BS} - \rho \ddot{u}) \quad \dots\dots\dots (3.11)$$

Substituting Eqn. (3.9) into Eqn. (3.10)

$$\sigma = D(Bd^e - \varepsilon_0) + \sigma_0 \quad \dots\dots\dots (3.12)$$

Substituting from Eqn. (3.8 a),(3.9 a), (3.10) and (3.11) in to Eqn.(3.7) for an element

$$\begin{aligned} \delta \pi_p = & \delta d^{eT} \iiint B^T DB dv_e d^e - \delta d^{eT} \iiint B^T D \varepsilon_0 dv_e + \delta d^{eT} \iiint B^T \sigma_0 dv_e \\ & - \delta d^{eT} \iint \overline{N^T} F_\tau d\tau_e - \delta d^{eT} \iiint \overline{N^T} F_B dv_e = 0 \end{aligned}$$

$$\begin{aligned} \delta \pi_p^e = & \delta [d^{eT} \{ \frac{1}{2} \iiint B^T DB dv_e d^e - \iiint B^T D \varepsilon_0 dv_e + \iiint B^T \sigma_0 dv_e \\ & - \iint \overline{N^T} F_\tau d\tau_e - \iiint \overline{N^T} F_B dv_e \}] = 0 \end{aligned}$$

$$\begin{aligned} \pi_p^e = & [d^{eT} \{ \frac{1}{2} \iiint B^T DB dv_e d^e - \iiint B^T D \varepsilon_0 dv_e + \iiint B^T \sigma_0 dv_e \\ & - \iint \overline{N^T} F_\tau d\tau_e - \iiint \overline{N^T} F_B dv_e \}] = 0 \quad \dots\dots\dots (3.13) \end{aligned}$$

System equation is given by

$$\frac{\partial \pi_p^e}{\partial d^e} = \sum_{e=1}^{ne} \frac{\partial \pi_p^e}{\partial d^e} = 0 \quad \dots\dots\dots (3.14)$$

Element equation after substituting Eqn. (3.11) in (3.13) and using Eqn. (3.14)

$$\frac{\partial \pi_p^e}{\partial d^e} = \iiint B^T DB dv_e d^e - \iiint B^T D \varepsilon_0 dv_e + \iiint B^T \sigma_0 dv_e$$

$$- \iint \overline{N}^T F_\tau d\tau_e - \iiint \overline{N}^T F_B dv_e + \iiint \overline{N}^T \rho \overline{N} dv_e \ddot{d}^e \quad \dots\dots\dots (3.15)$$

Let

$$[K_e] = \text{Element Stiffness Matrix} = \iiint B^T DB dv_e \quad \dots\dots\dots (3.16)$$

$$[M_e] = \text{Element mass matrix} = \iiint \overline{N}^T \rho \overline{N} dv_e \quad \dots\dots\dots (3.17)$$

(v) Equivalent nodal forces

$$\{F_{\epsilon 0}\}^e = \iiint B^T D \epsilon_0 dv_e$$

$$\{F_{\sigma 0}\}^e = - \iiint B^T \sigma_0 dv_e \quad \dots\dots\dots(3.18)$$

$$\{F_\tau\}^e = \iint \overline{N}^T F_\tau d\tau_e \quad \dots\dots\dots(3.19)$$

$$\{\overline{F}_{BS}\}^e = \iiint \overline{N}^T F_B d\tau_e \quad \dots\dots\dots(3.20)$$

$$\{F_{BS}\}^e = \iiint \overline{N}^T F_B d\tau_e \quad \dots\dots\dots(3.21)$$

Let $\{F\}^e = \{F_{\epsilon 0}\}^e + \{F_{\sigma 0}\}^e + \{F_\tau\}^e + \{\overline{F}_{BS}\}^e \quad \dots\dots\dots (3.22)$

Substituting from Eqn. (3.16) to (3.22) in Eqn. (3.15)

$$\sum_{e=1}^{ne} ([M]^e \{\ddot{d}\}^e + [K]^e \{d\}^e - \{F\}^e) = 0 \quad \dots\dots\dots (3.23)$$

System equation after assembly is in the following form

$$[M]\{\ddot{d}\} + [K]\{d\} = \{F\} \quad \dots\dots\dots (3.24)$$

Where

$$[M] = \sum_{e=1}^{ne} [M]^e = \text{System mass matrix} \quad \dots\dots\dots (3.25)$$

$$[K] = \sum_{e=1}^{ne} [K]^e = \text{System stiffness matrix} \quad \dots\dots\dots (3.26)$$

$$\{F\}^e = \sum_{e=1}^{ne} (\{F_{\epsilon 0}\}^e + \{F_{\sigma 0}\}^e + \{F_\tau\}^e + \{\overline{F}_{BS}\}^e) \quad \dots\dots\dots (3.27)$$

=System nodal force matrix

3.3 FINITE ELEMENT ANALYSIS OF 2-D QUARDILATERAL ELEMENTS

Let number of nodes per element = ne

1. Displacement function

$$u = \sum_{i=1}^{ne} N_i u_i^e,$$

$$v = \sum_{i=1}^{ne} N_i v_i^e$$

Where

N_i = shape functions

$$= N_i(\xi, \eta) \quad (i=1,2,\dots,ne)$$

In matrix form

$$u = d = \begin{Bmatrix} u \\ v \end{Bmatrix} = \begin{bmatrix} N_1 & 0 & \dots & N_{ne} \\ 0 & N_1 & \dots & 0 \end{bmatrix} \begin{Bmatrix} u_1 \\ v_1 \\ \vdots \\ u_{ne} \\ v_{ne} \end{Bmatrix}$$

$$u = [IN_1 \quad IN_2 \quad \dots \quad IN_e] \{d\}^e = \bar{N} d^e$$

2. (a) Co-ordinate Transformation

$$x = \sum_{i=1}^{ne} N_i x_i$$

$$y = \sum_{i=1}^{ne} N_i y_i$$

(b) Jacobian Matrix

$$[J] = \begin{bmatrix} \partial x / \partial \xi & \partial y / \partial \xi \\ \partial x / \partial \eta & \partial y / \partial \eta \end{bmatrix}$$

$$= \begin{bmatrix} \sum (\partial N_i / \partial \xi) x_i & \sum (\partial N_i / \partial \xi) y_i \\ \sum (\partial N_i / \partial \eta) x_i & \sum (\partial N_i / \partial \eta) y_i \end{bmatrix}$$

(c) Cartesian Derivatives

$$\text{Now } \begin{bmatrix} \partial N_i / \partial \xi \\ \partial N_i / \partial \eta \end{bmatrix} = [J] \begin{Bmatrix} \partial N_i / \partial x \\ \partial N_i / \partial y \end{Bmatrix}$$

$$\begin{Bmatrix} \partial N_i / \partial x \\ \partial N_i / \partial y \end{Bmatrix} = [J]^{-1} \begin{Bmatrix} \partial N_i / \partial \xi \\ \partial N_i / \partial \eta \end{Bmatrix} \quad (i = 1, 2, 3, \dots, ne)$$

(d) Strain-displacement Relations

$$\varepsilon = \begin{Bmatrix} \varepsilon_x \\ \varepsilon_y \\ \gamma_{xy} \end{Bmatrix} = \begin{Bmatrix} \partial u / \partial x \\ \partial v / \partial y \\ \partial u / \partial y + \partial v / \partial x \end{Bmatrix} = \begin{Bmatrix} \sum (\partial N_i / \partial x) u_i^e \\ \sum (\partial N_i / \partial y) v_i^e \\ \sum (\partial N_i / \partial y) u_i^e + \sum (\partial N_i / \partial x) v_i^e \end{Bmatrix}$$

$$\begin{bmatrix} \partial N_1 / \partial x & 0 & 0 & \text{-----} \\ 0 & \partial N_1 / \partial y & 0 & \text{-----} \\ \partial N_1 / \partial y & \partial N_1 / \partial x & 0 & \text{-----} \end{bmatrix} \begin{Bmatrix} u_1 \\ v_1 \\ \downarrow \\ \downarrow \end{Bmatrix}$$

$$\varepsilon = [[B_1] \quad [B_2] \quad \dots \quad [B_{ne}]] \{d\}^e = B d^e$$

$$[B_i] = \begin{bmatrix} \partial N_i / \partial x & 0 & 0 \\ 0 & \partial N_i / \partial y & 0 \\ \partial N_i / \partial y & \partial N_i / \partial x & 0 \end{bmatrix} \quad (i = 1, 2, 3, \dots, ne)$$

3. Stress –strain Relations

$$\sigma = D(\varepsilon - \varepsilon_0) + \sigma_0$$

4. Element stiffness Matrix

$$\begin{aligned} [K]^e &= \int_{-1}^1 \int_{-1}^1 B^T D B t_e dA_e \\ &= \int_{-1}^1 \int_{-1}^1 B^T D B t_e d\xi d\eta \end{aligned}$$

3.4 CONCEPT OF COMPOSITE LAMINAS

Due to rising demand for increase in strength, stiffness and other mechanical properties, composite materials are widely used as engineering materials. Composite laminates consists of several layers of thin films (of same or different material) at some angle as shown in figure 3.1.

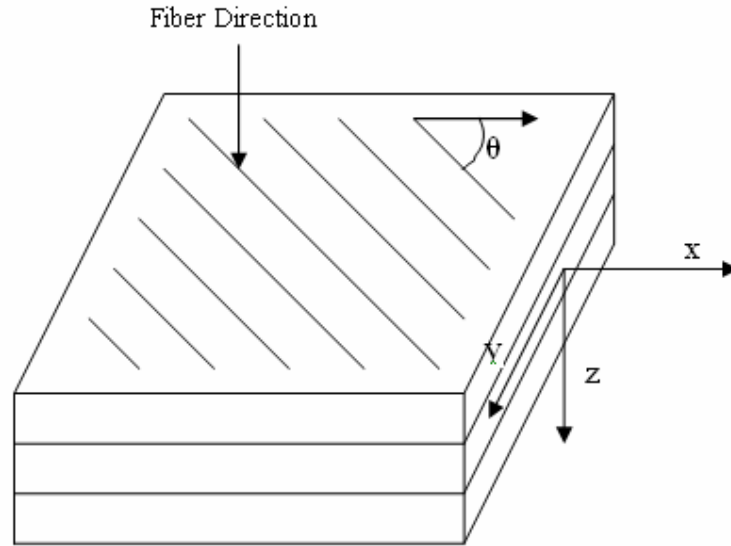


Figure 3.1 Composite Lamina Structure

Stress strain relationship for a lamina is given by:

$$\begin{bmatrix} \sigma_1 \\ \sigma_2 \\ \tau_{12} \end{bmatrix} = \begin{bmatrix} Q_{11} & Q_{12} & 0 \\ Q_{12} & Q_{22} & 0 \\ 0 & 0 & Q_{66} \end{bmatrix} \begin{bmatrix} \varepsilon_1 \\ \varepsilon_2 \\ \gamma_{12} \end{bmatrix} \quad \dots\dots\dots (3.28)$$

Where, Q_{ij} are the reduced stiffness coefficients. These coefficients are related to engineering constants as

$$Q_{11} = \frac{E_1}{1 - \nu_{21}\nu_{12}} \quad \dots\dots\dots (3.28 \text{ a})$$

$$Q_{12} = \frac{\nu_{12}E_2}{1 - \nu_{21}\nu_{12}} \quad \dots\dots\dots (3.28 \text{ b})$$

$$Q_{22} = \frac{E_2}{1 - \nu_{21}\nu_{12}} \quad \dots\dots\dots (3.28 \text{ c})$$

$$Q_{66} = G_{12} \quad \dots\dots\dots(3.28 \text{ d})$$

Where

E_1 =Longitudinal Young's modulus (in direction 1)

E_2 =Transverse Young's modulus (in direction 2)

ν_{12} =Major Poisson ratio

G_{12} = in plane shear modulus.

Generally, a laminate does not consist only of unidirectional laminas because of their low stiffness and mechanical properties in the transverse direction .Hence in most laminates; some laminas are placed at an angle. It is thus necessary to develop the stress-strain relationship for an angle lamina.

In Figure (3.2) x-y Coordinate system shows the global coordinate system, whereas 1-2 shows local coordinate system.

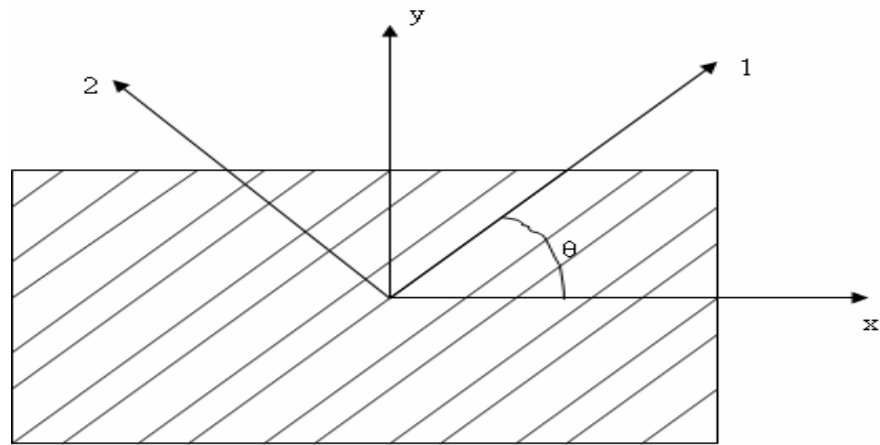


Figure 3.2 Local and Global Coordinate System

The global and local stresses in an angle lamina are related to each other through the angle of lamina, θ as

$$\begin{bmatrix} \sigma_x \\ \sigma_y \\ \tau_{xy} \end{bmatrix} = [T]^{-1} \begin{bmatrix} \sigma_1 \\ \sigma_2 \\ \tau_{12} \end{bmatrix}$$

Where $[T]$ is called the transformation matrix and is defined as

$$[T]^{-1} = \begin{bmatrix} c^2 & s^2 & -2sc \\ s^2 & c^2 & 2sc \\ sc & -sc & c^2 - s^2 \end{bmatrix}$$

$$[T] = \begin{bmatrix} c^2 & s^2 & 2sc \\ s^2 & c^2 & -2sc \\ -sc & sc & c^2 - s^2 \end{bmatrix}$$

And

$$c = \cos(\theta)$$

$$s = \sin(\theta)$$

Similarly the global and local strains are related through the transformation matrix which can be written as

$$\begin{bmatrix} \varepsilon_1 \\ \varepsilon_2 \\ \gamma_{12} \end{bmatrix} = [R][T][R]^{-1} \begin{bmatrix} \varepsilon_x \\ \varepsilon_y \\ \gamma_{xy} \end{bmatrix}$$

Where $[R]$ is Reuter matrix and is given by

$$R = \begin{bmatrix} 1 & 0 & 0 \\ 0 & 1 & 0 \\ 0 & 0 & 2 \end{bmatrix}$$

On arranging all these global stress-strain (for angled lamina) can be related as

$$\begin{bmatrix} \sigma_x \\ \sigma_y \\ \tau_{xy} \end{bmatrix} = [T]^{-1}[Q][R][T][R]^{-1} \begin{bmatrix} \varepsilon_x \\ \varepsilon_y \\ \gamma_{xy} \end{bmatrix}$$

On multiplication we get

$$\begin{bmatrix} \sigma_x \\ \sigma_y \\ \tau_{xy} \end{bmatrix} = \begin{bmatrix} \overline{Q}_{11} & \overline{Q}_{12} & \overline{Q}_{16} \\ \overline{Q}_{12} & \overline{Q}_{22} & \overline{Q}_{26} \\ \overline{Q}_{16} & \overline{Q}_{26} & \overline{Q}_{66} \end{bmatrix} \begin{bmatrix} \varepsilon_x \\ \varepsilon_y \\ \gamma_{xy} \end{bmatrix} \quad \dots\dots\dots (3.29)$$

Where Q_{ij} are called the elements of the transformed reduced stiffness matrix $[Q]$ and are given by

$$\overline{Q}_{11} = Q_{11}c^4 + Q_{22}s^4 + 2(Q_{12} + 2Q_{66})s^2c^2 \quad \dots\dots\dots (3.29 a)$$

$$\overline{Q}_{12} = (Q_{11} + Q_{22} - 4Q_{66})s^2c^2 + Q_{12}(c^4 + s^4) \quad \dots\dots\dots(3.29b)$$

$$\overline{Q}_{22} = Q_{11}s^4 + Q_{22}c^4 + 2(Q_{12} + 2Q_{66})s^2c^2 \quad \dots\dots\dots(3.29c)$$

$$\overline{Q}_{16} = (Q_{11} - Q_{12} - 2Q_{66})c^3s - (Q_{22} - Q_{12} - 2Q_{66})s^3c \quad \dots\dots\dots(3.29d)$$

$$\overline{Q}_{26} = (Q_{11} - Q_{12} - 2Q_{66})cs^3 - (Q_{22} - Q_{12} - 2Q_{66})c^3s \quad \dots\dots\dots(3.29e)$$

$$\overline{Q}_{66} = (Q_{11} + Q_{22} - 2Q_{12} - 2Q_{66})s^2c^2 + Q_{66}(s^4 + c^4) \quad \dots\dots\dots(3.29f)$$

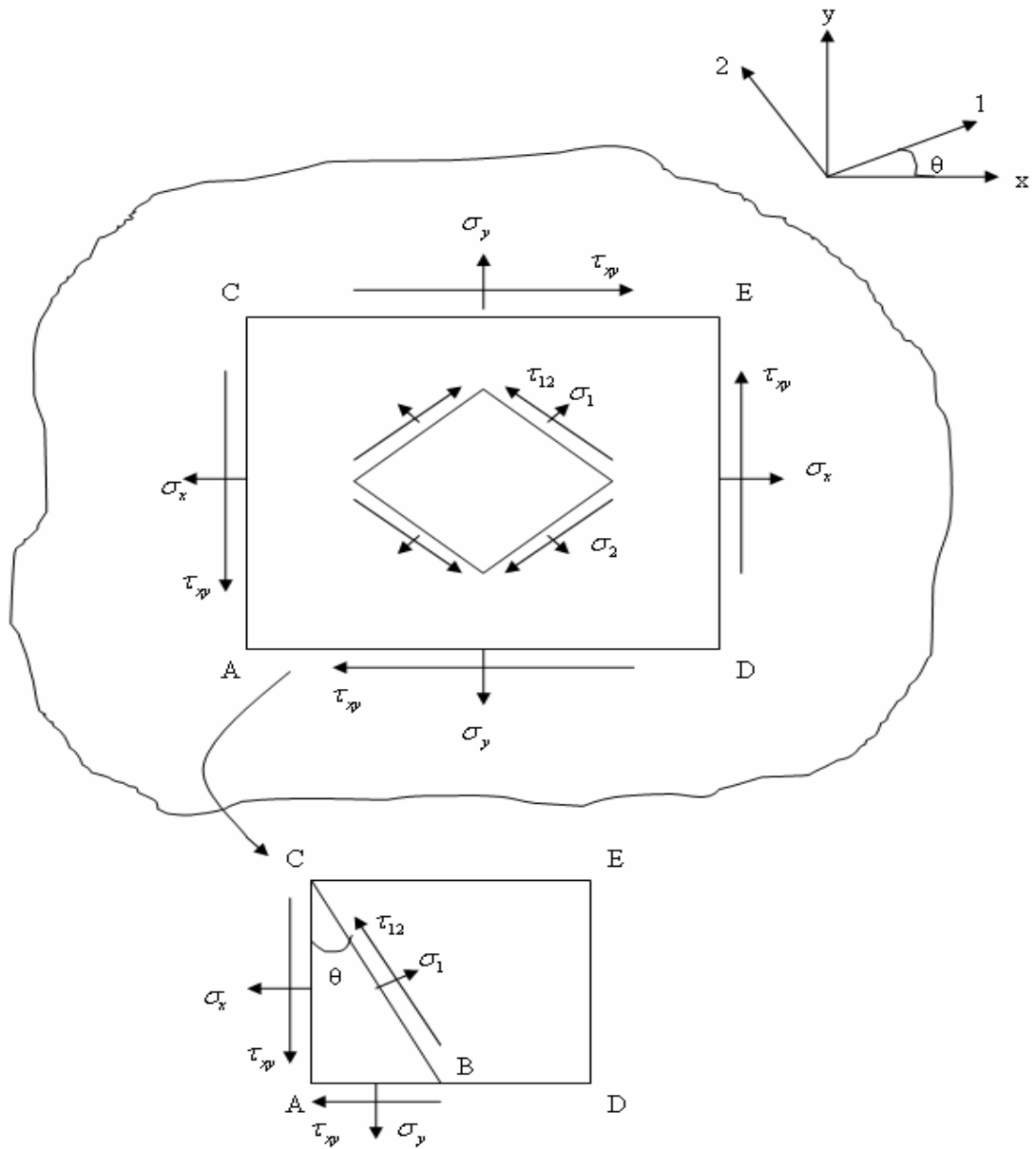


Figure 3.3 Transformation of Local Coordinate System To Global Coordinate System

3.5 LAMINA SUBJECTED TO IN-PLANE LOADING

For a symmetric laminate subjected to in-plane loading only (no bending moments), the laminate strain increments $\{\Delta\varepsilon\}_{xy}$ (which will be same in each ply) can be related to the in-plane force increments $\{\Delta N\}_{xy}$ applied to the laminate by

$$\{\Delta N\}_{xy} = [A]\{\Delta\varepsilon\}_{xy} \quad \dots\dots\dots (3.30)$$

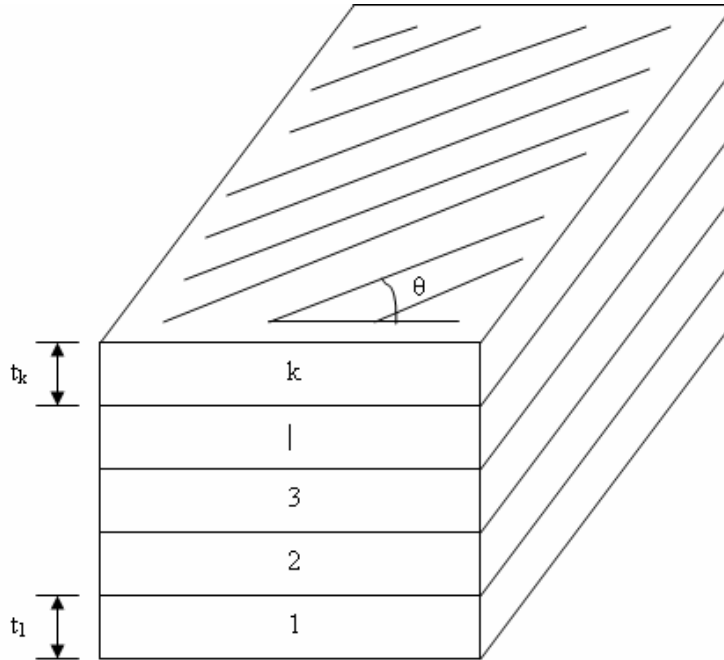


Figure 3.4 Composite Material Stack

Where $[A]$ is the conventional extensional stiffness matrix, and can be expressed as

$$[A] = \sum_{k=1}^n [\bar{Q}]_k t_k \quad \dots\dots\dots(3.31)$$

Where

'n' is the number of plies in the laminate and t_k are the thickness of the k^{th} ply.

3.6 DAMAGE ANALYSIS

It is well known that composite materials can experience a variety of forms of damage, including matrix cracking, fiber fracture or buckling and fiber/matrix debonding. The mode in which a particular ply may fail can depend on the geometry of the component, the orientation and stacking sequence of the plies, and the direction of external loading. Since the failure of an individual ply

causes a loss of load-carrying capacity (reduction in stiffness) of that ply, a redistribution of stresses will occur in the failed ply and surrounding plies.

Due to the complex nature of failure modes in fiber reinforced composite laminates, interactions between stresses can significantly alter the load-carrying capacity of individual plies. Failure criteria that do not account for interaction effects have often been shown to be in poor agreement with experiment.

Hashin proposed four separate criteria to predict failure of unidirectional fiber composites (plies) in an arbitrary state of plane stress. These criteria identify four possible modes of failures of a ply: longitudinal tensile failure, longitudinal compressive failure, transverse tensile failure, and transverse compressive failure.

These can be expressed as follows:

Longitudinal tension:

$$\left[\frac{\sigma_1}{X_t} \right]^2 + \left[\frac{\sigma_{12}}{S_L} \right]^2 = 1 \quad \dots\dots\dots (3.32)$$

Longitudinal compression: $\sigma_1 = X_c$ \dots\dots\dots (3.33)

Transverse tension:

$$\left[\frac{\sigma_2}{Y_t} \right]^2 + \left[\frac{\sigma_{12}}{S_L} \right]^2 = 1 \quad \dots\dots\dots (3.34)$$

Transverse compression:

$$\left[\frac{\sigma_2}{2S_t} \right]^2 + \left\{ \left[\frac{Y_c}{2S_T} \right]^2 - 1 \right\} \left[\frac{\sigma_2}{Y_c} \right] + \left[\frac{\sigma_{12}}{S_L} \right]^2 = 1 \quad \dots\dots\dots (3.35)$$

Where

X_t and X_c are the longitudinal tensile and compressive strengths of a unidirectional lamina, Y_t and Y_c are the transverse tensile and compressive strength of a unidirectional lamina, and S_L and S_T are the longitudinal and transverse shear strengths.

Using these criteria, once $\sigma_1, \sigma_2, \text{ and } \sigma_{12}$ have been calculated in each lamina, Failure of a ply is predicted if any of equations are satisfied.

Once a ply fails at some point in a laminate, that ply experiences a loss of load-carrying capacity, or a reduction in stiffness, in the damaged area. The magnitude and direction of this stiffness degradation are dependent on the failure mechanisms, and hence mode of failure, of a ply. In most cases, ply stiffness were reduced only in the direction of failure.

If ply fails under longitudinal tension or transverse tension the material properties are degraded as: $E_1, \nu_{12}, \nu_{21} \rightarrow 0$ else if it fails under transverse tension or transverse compression then $E_2, G_{12}, \nu_{12}, \nu_{21} \rightarrow 0$

The second criterion used to simulate damage is Hoffman criteria formed by adding linear terms to Tsai Hill's equation. According to it a ply fails if

$$\frac{\sigma_1^2}{X_t X_c} + \frac{\sigma_1 \sigma_2}{X_t X_c} - \frac{\sigma_2^2}{Y_t Y_c} + \frac{X_t + X_c}{X_T X_C} \sigma_1 + \frac{Y_t + Y_c}{Y_t Y_c} \sigma_2 + \frac{\tau_{12}^2}{S^2} = 1 \quad \dots\dots\dots (3.36)$$

is satisfied, However the mode of failure is determined by θ_f , the angle of first failure node. if

- $0^\circ \leq |\theta_f| \leq 15^\circ$ Indicates failure under bearing mode
- $30^\circ \leq |\theta_f| \leq 60^\circ$ Under shear-out mode
- $75^\circ \leq |\theta_f| \leq 90^\circ$ Under net-tension mode

The Material Properties are reduced as $E_1, E_2, G_{12}, \nu_{12}, \nu_{21} \rightarrow 0$

The above presented analysis forms the basis for construction of Solution Scheme given in chapter 4.

CHAPTER 4

SOLUTION SCHEME

For analyzing the damage growth in composite laminate a programme based on analysis presented in previous chapter has been developed. The programming work has been performed in Visual C++. In the following section, structure of the computer program developed is explained in brief.

4.1 EQUATION SOLUTION SCHEME

For a discretized continuum, the system equation presents a set of algebraic equations. Solutions of these simultaneous equations form a vital part of any finite element process. In the case of damage analysis of composite laminates, the system equation solution scheme is more important as numbers of equations are very large.

Here, band solver technique has been used. In band solver technique, the final assembly matrix has been converted into a banded matrix. In banded matrix, all the nonzero elements are contained within a band; outside the band all elements are zero. The band width was calculated using connectivity data for all elements known as half-bandwidth.

4.2 COMPUTATIONAL PROCEDURES

Following steps are being used to carry out Finite Element analysis:

4.2.1 Damage Analysis

The specific computational procedure performed by finite element code is explained in the following steps

1. Input model geometry, boundary conditions, material properties, etc. Construct initial (undamaged and unloaded) stiffness matrix $[K]$.
2. Apply external nodal force increment $\{\Delta f\}_i$
3. Solve for displacements, strains, and stresses using current force increments using general equation $[K]_i \{\Delta u\} = \{\Delta f\}$
4. Using the current stress state, check for element failure from eqn (3.32) to eqn. (3.35)(Hashin Failure Criteria) or eqn. 3.36 (Hoffman Failure Criteria),

if no failures are detected, return to step 2 with the next load increment. Otherwise, proceed to step 5.

5. Using the property degradation model modify the inverse compliance tensors of the damaged elements as indicated in Equation.
6. Recalculate $[K]_t$ and $\{f\}_t$ for damaged laminate and return to step 2.

4.3 PROGRAM STRUCTURE

The program has been developed in the modular form such that various finite element operations are being performed by separate subroutines. Figure 4.1 shows the organization of program developed. The basic finite element steps are performed by primary subroutines which rely on auxiliary subroutines to carry out secondary operations. An auxiliary subroutine may be called by more than once by primary subroutine.

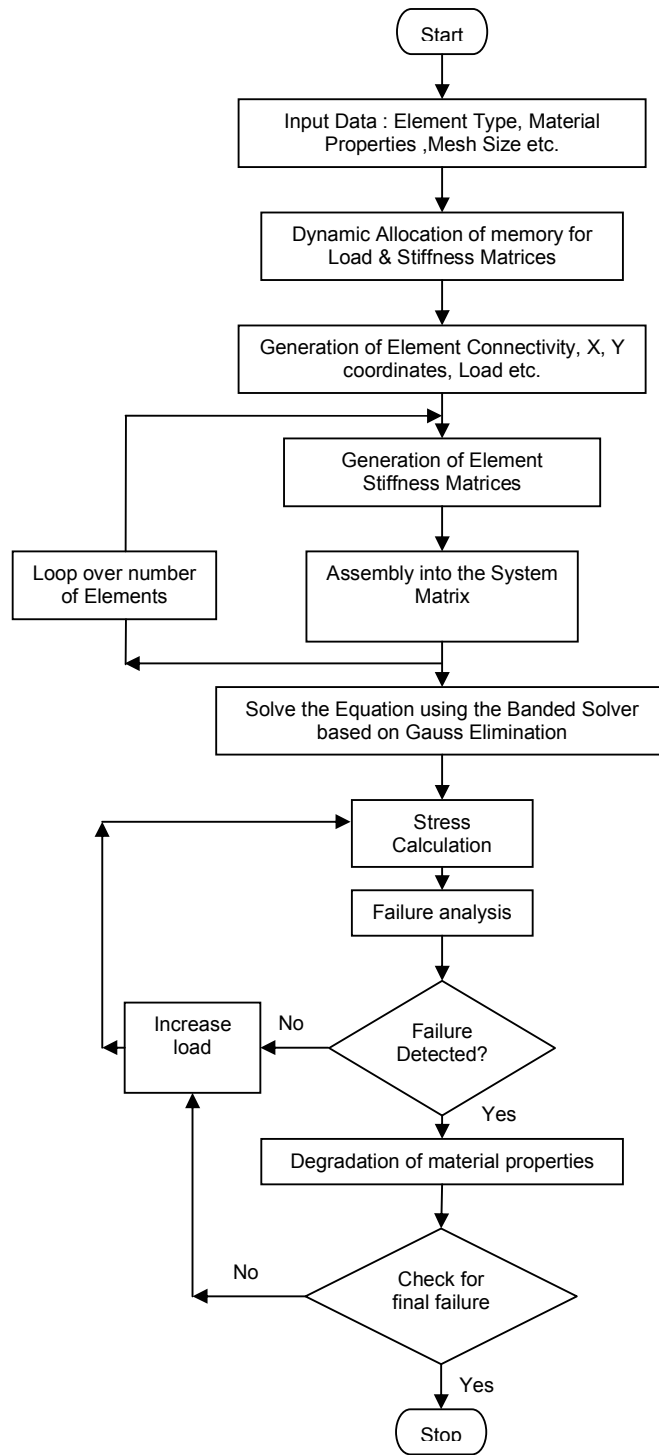


Figure 4.1 Flow Chart for the Main Program

The Function Of Each Subroutine Is Described In Brief As Follow:

- INPUT() This function reads data from file for co-ordinates, connectivity, loads, material properties etc.
- INTEG() This function calls the value at integration points.
- BANDWIDTH() This function calculates the bandwidth for memory allocation and calculation purposes.
- LOAD() This function distributes the applied load according to the given problem.
- DMATRIX() This function calculates stress-strain relationship matrix 'D' for laminate, which is given by $\sum_{k=1}^n [Q_{ij}]_k t_k$ where Q_{ij} is the transformed stiffness matrix & t_k is the thickness of individual lamina.
- DBMAT() This function calculates 'DB' matrix & also the determinant of jacobian matrix, |J|. Figure 4.3 shows flow chart for calculating jacobian matrix, its inverse and for finding global derivative.
- ELE_STIFF() This function calculates stiffness matrix for each element using equation $\int_{-1}^1 \int_{-1}^1 B^T DB |J| d\xi d\eta$. Figure 4.2 shows flow chart for calculating element stiffness matrix.
- BANSOL() This function solves the system equation $[K]\{u\} = \{F\}$
- STRESS() This function calculates the stresses within an element using the equation $\sigma = DBq$, where 'q' is the displacement vector for corresponding element.
- COMP_FRAC() This function checks the stability of an element under longitudinal as well as transverse direction using Hashin's criteria for failure of elements
- COMP_FRACHOFF() This function checks the stability of an element using Hoffman Failure Criteria.

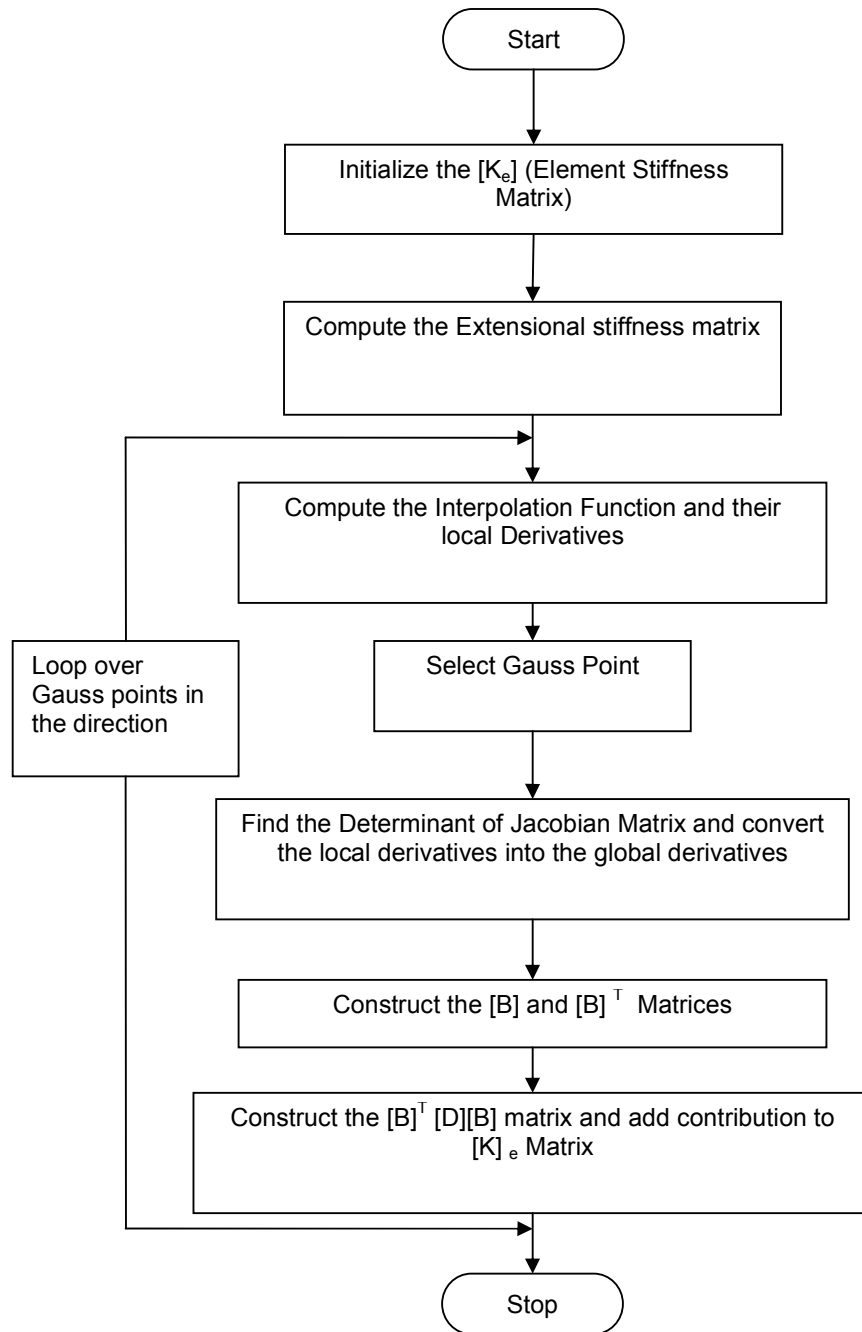


Figure 4.2 Flow Chart for Calculating Elemental Stiffness Matrix

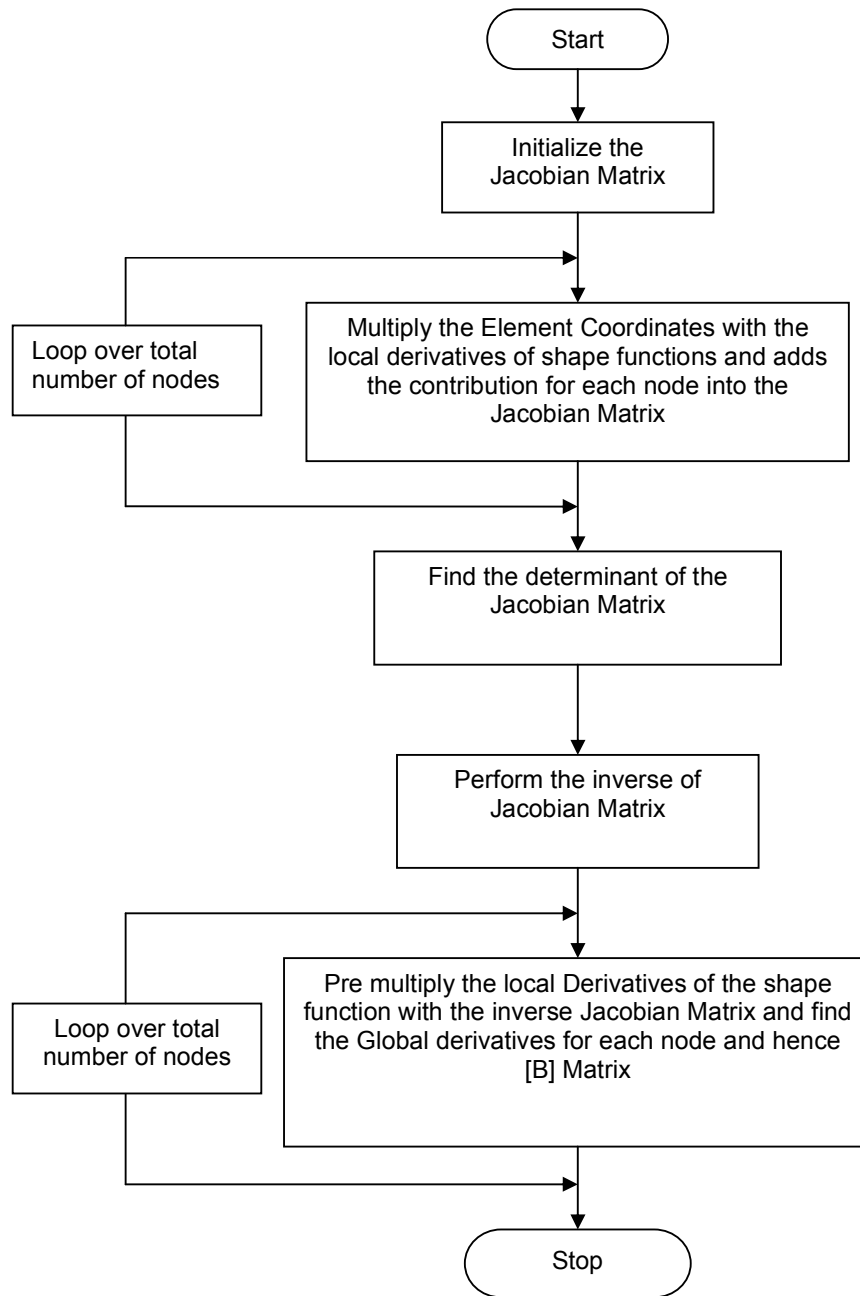


Figure 4.3 Flow Chart for Calculation Of Jacobian Matrix

5.1 INTRODUCTION TO PROBLEM

For the present study, the damage analysis of laminated structure subjected to static bearing load has been performed using finite element code. The material used in this study is a carbon fiber reinforced epoxy matrix composite. The analysis is conducted using the single-hole, pinned joint specimen shown in Figure 5.1. The dimensions for various configurations are as per Table 5.1.

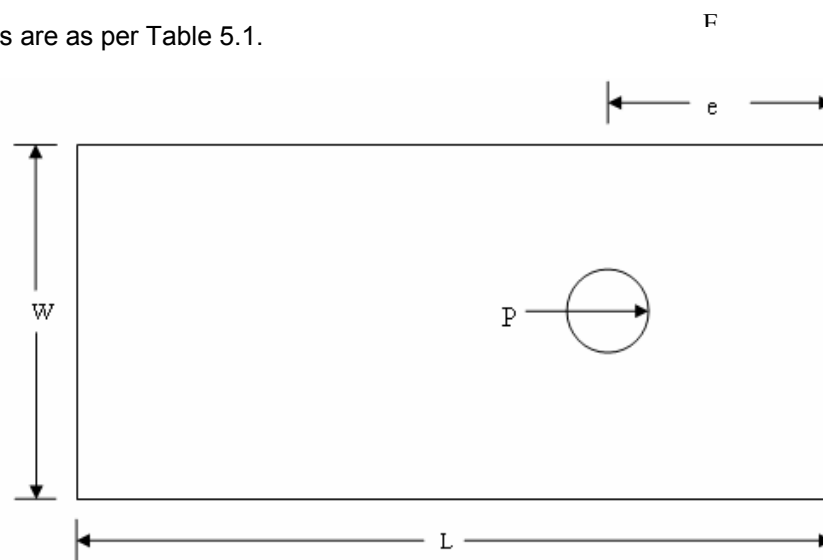


Figure 5.1 Specimen Configuration

Table 5.1 Specimen Dimensions

configuration	L (mm)	W (mm)	E (mm)
Case1(E/D=1)	70	20	5
Case 2 (E/D=2)	70	20	10
Case 3(E/D=3)	70	20	15
Case 4(E/D=4)	70	20	20
Case 5(E/D=5)	70	20	25

Where D is the diameter of hole in mm.

Table 5.2 Elastic Material Constants

Material	E1	E2	G12	v 12
Carbon -epoxy	100	100	6.12	0.4

The material parameters required by the damage analysis used in this study are shown in Table 5.2.

Table 5.3 Material Parameters for Damage Analysis

Material	Xt	Xc	Yt	Yc	SL	ST
Carbon -epoxy	850	700	35	130	60	60

5.2 FINITE ELEMENT MESHING

The finite element mesh used in this study is shown in figure 5.3. with a higher concentration of elements in the vicinity of the bolt hole to provide better accuracy in the region of high stress gradients. All elements are two-dimensional, four-node, quadrilateral elements.

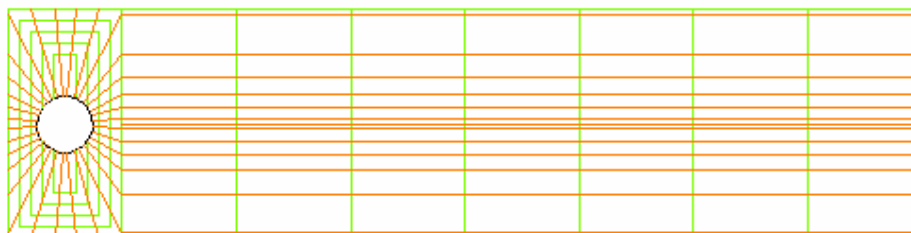


Figure 5.2(a). Case1 ($E/D=1, W/D=4$)

For the first case the value of E is 5 and W is 20. The number of nodes generated for it is 134 and domain is divided into 100 elements.

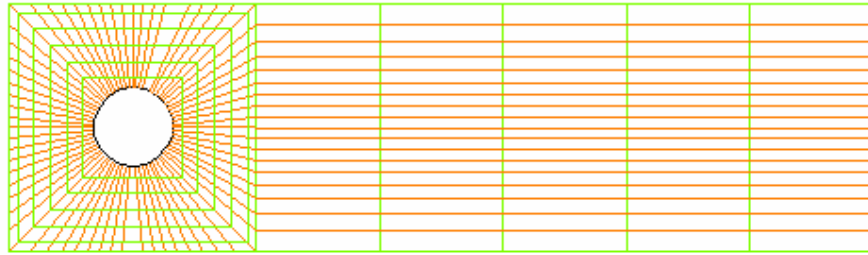


Figure 5.2(b). Case2 ($E/D=2$, $W/D=4$)

Then for second case for which the value of E is 10 and W is 20 the number of nodes generated are 141 and 106 elements are formed.

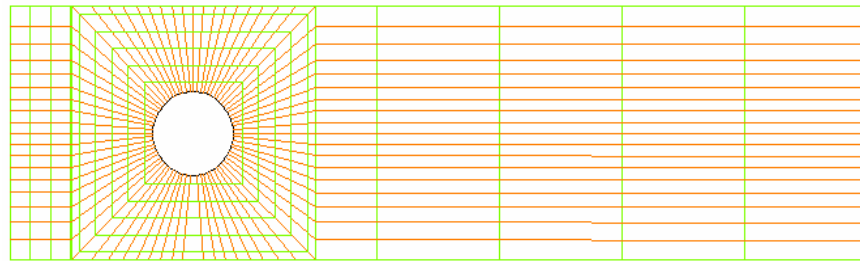


Figure 5.2(c). Case3 ($E/D=3$, $W/D=4$)

For case 3 the value of E is increased to 15 and W is kept same. 162 nodes and 124 elements are being generated for this case.

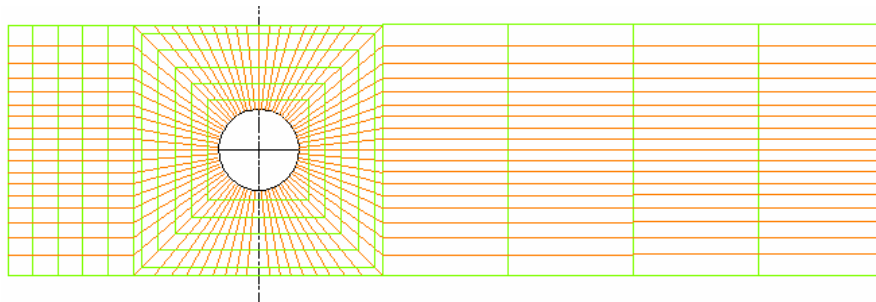


Figure 5.2(d). Case4 ($E/D=4$, $W/D=4$)

With an increment in E it becomes 20 and W is kept as 20. The numbers of nodes generated for this case are 176 and the numbers of elements are 136.

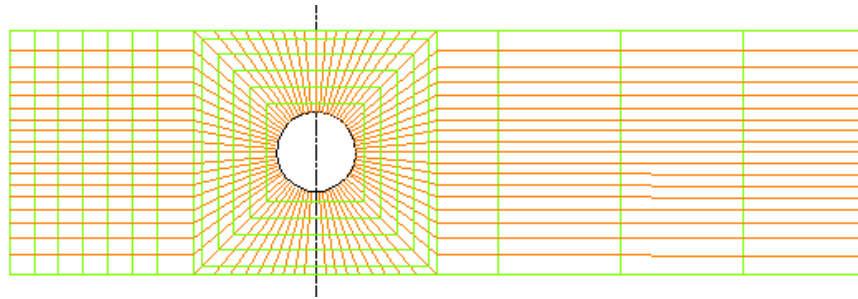


Figure 5.2(e). Case5 (E/D=5, W/D=4)

For the final case the value of E is kept as 25 and W is equal to 20. The number of nodes generated for this case are 197 and domain is divided into 154 elements.

Figure 5.2 Finite Element Discretization Of The Specimen

5.3 BOUNDARY CONDITIONS

A boundary conditions used in the Finite Element Analysis are shown below. To determine the exact distribution of T_i , a cosine normal load distribution is assumed [4]. with this approximation T_i becomes:

$$T_i = \frac{-4P}{\pi D} n_i \cos \theta$$

Where

T_i =Load Distribution Function.

P=Applied Load.

D=Diameter of the hole.

n_i =Unit vector normal to surface.

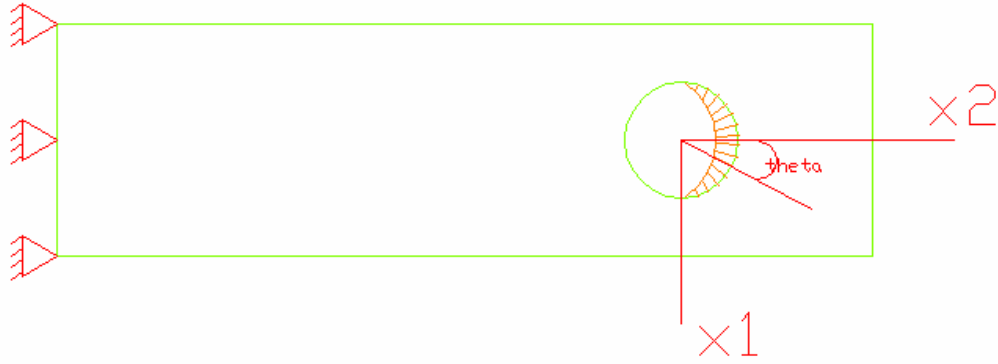


Figure 5.3 Boundary Conditions and Forces Applied to the Specimen in Finite Element Model

One of the edges of the plate has been fixed as shown in Figure 5.3 and the displacements at these nodes are zero. The load distribution is applied to the nodes at the circumference of hole. Linear two dimensional modeling implies assumptions such as the thickness of plate must be small compared with the plate width and length [12]. To simplify the contact between the pin and the laminated plate, the pin circumference is modeled as a rigid surface and surface of the hole is modeled as a deformable surface. This simplification is justified because the primary objective of this analysis is to study the damage progression in the plate only. Using this assumption both the friction and pin clearance can be neglected [6].

5.4 VALIDATION OF WORK

For validation of present work, the developed program has been executed for a case shown in figure 5.4 below. The result obtained are in total conformance with the problem undertaken [12].

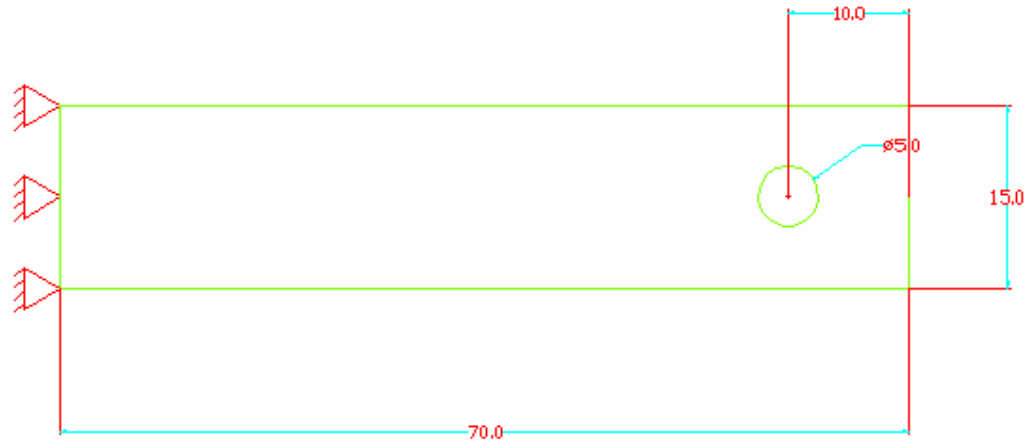


Figure 5.4 Problem Taken For Validation

($E/D=2$, $W/D=3$)

The value of E is 10 and W is 15. The number of nodes generated are 190 and domain is divided into 148 elements. The Initial applied load is 100 N. load increment is set as 100N .The first failure is found to occur at a load of 400 N. The progress of damage due to increase in load has been shown in figure 5.6. The damage initiated at node number 47 under fiber compressive mode. In next load increment element number 48, 53, 71 failed under fiber compressive, fiber tensile and matrix tensile mode. No elements failed in next load increment. At a load of 600N element number 70, 58, 46 and 41 failed. At a load value of 1000 N the elements failed are 0. At value of 1500 N, 33 elements failed. The damage progression is shown in figure 5.6. The failure starts from the hole circumference and propagates to the outer edge of plate. The ultimate failure load of 2700 N is obtained.

Failure Modes: +: Fiber Tensile ×: Fiber Compressive. Δ: Matrix Tensile ∴: Matrix Compressive H: Hoffman

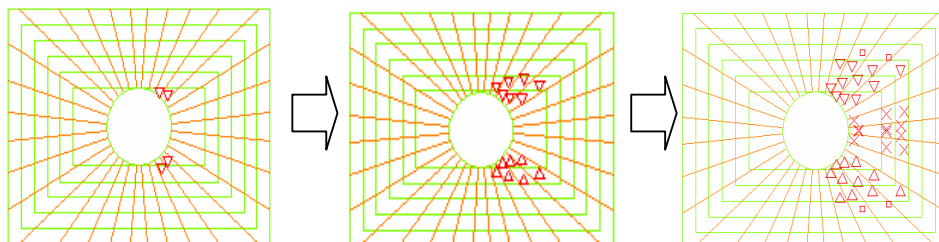


Figure 5.5 Illustration of Damage Propagation at Different Load Steps

Similar sort of work has been carried out for case 4 ($E/D=4$, $W/D=4$). The results Obtained For different fiber angle are shown in figure 5.7



Figure 5.6 Illustration of Damage Propagation ($E/D=4$; $W/D=4$; $\Theta=0$)

Using Hashin's Criteria For the above case the first element to fail is 28. Then the next five elements which failed are 22, 23, 28, 34, 38. Whereas the damage was found to initiate from node number 30 and the next five elements to fail are element number 31, 32, 37, 40, 41 using Hoffman criteria.

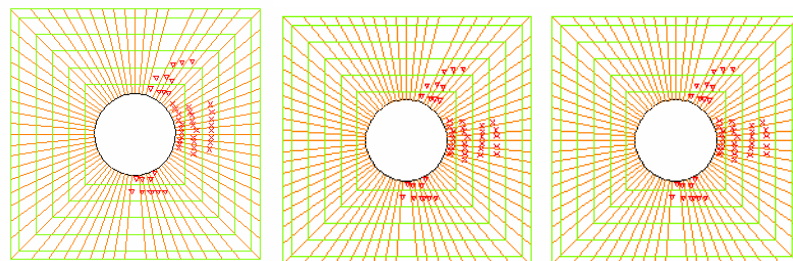


Figure 5.7 Illustration of Damage Propagation

($E/D=4$; $W/D=4$; $\Theta=15$, $\Theta=30$, $\Theta=45$)

Figures 5.8 show the prediction of progressive damage in composite laminates at different load steps. The program has been executed for three different ply angles i.e. 0° , 30° and 45° . The damage progressions as well as failure modes have been obtained as shown. In the early stages of loading the composite plate behaves elastically with no indication of damage in material. As the load increases damage begins to appear near the stress concentration at the hole boundary. Damage initiates at about 45° with respect to the loading direction and propagates through the corner side of the laminate, due to loading of hole. Further loading causes damage growth leading to situation where the lamina cannot withstand more load i.e. where the point of ultimate failure has been reached. For final failure it has been selected the point where damage has spread to the outer edge of the specimen. For various fiber Angles the results obtained are as shown in table 5.4

Table 5.4 Comparison of Results

Θ	Result	Reference Results		Results Obtained	
		Hashin	Hoffman	Hashin	Hoffman
0	P(max)	2900	2800	2600	2300
15	P(max)	2450	1850	2100	1700
30	P(max)	1350	1250	1200	1200
45	P(max)	1100	1100	1100	1100

Comparison of Results is shown in figure below:

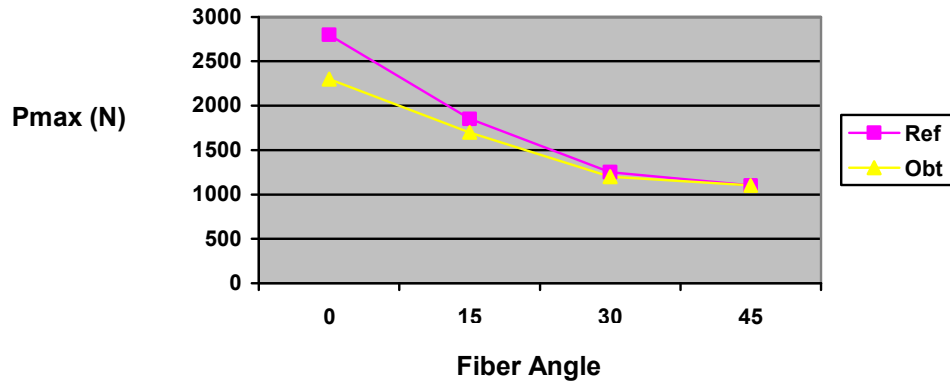


Figure 5.8 Comparison of Results (Hoffman Failure Criteria)

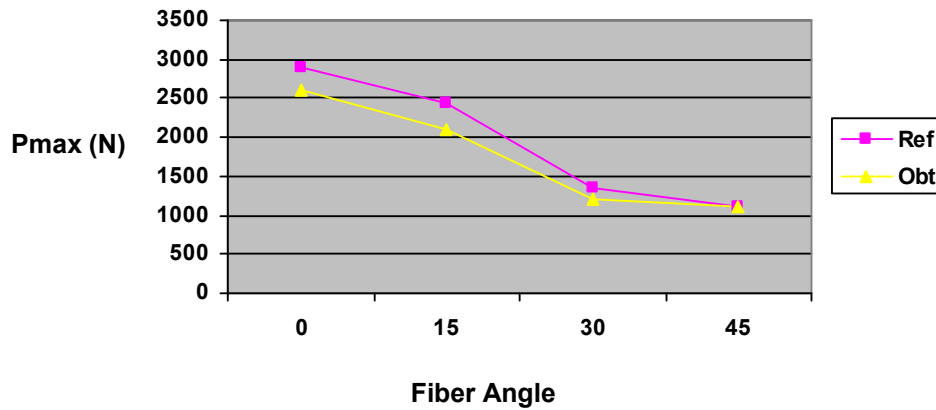


Figure 5.9 Comparison of Results (Hashin's Failure Criteria)

5.5 FAILURE STRENGTH OF LAMINATES WITH DIFFERENT LAY-UPS

Further study has been performed to Investigate the Failure Behavior of Carbon-epoxy composite for three different ply orientations $[0/\pm 45]_s$, $[90/\pm 45]_s$ and $[0/90/0/90/0/90]$ as shown in figure 5.10 below.

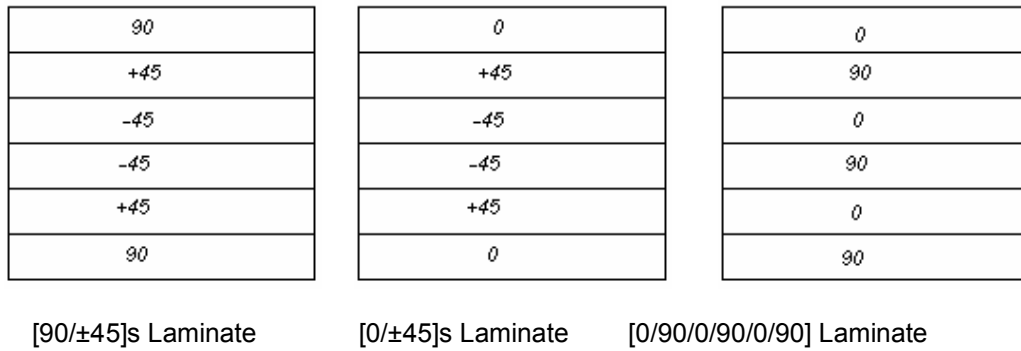


Figure 5.10 Laminate Schemes

Using the same FE code and boundary conditions an analysis of failure strengths of laminates with different lay-ups is carried out [13]. The material parameters used are given in Table 5.5. The results obtained for the first failure and final failure load for different E/D ratio and Laminate Schemes are shown next.

Table 5.5 Material Parameters for Damage Analysis of Laminate

Material	X _t	X _c	Y _t	Y _c	SL	ST
Carbon -epoxy	800	350	50	125	120	120

The Initial Failure load and final failure load for different E/D ratios were obtained and plotted. The values of first ply failure are shown in table 5.6.

Table 5.6 First Failure Load for Different Lay-Ups

Layup	First Failure Load				
	E/D=1	E/D=2	E/D=3	E/D=4	E/D=5
[0±45] _s	300	400	400	400	400

[90±45]s	300	400	300	300	300
[0/90/0/90/0/90]	300	200	300	300	300

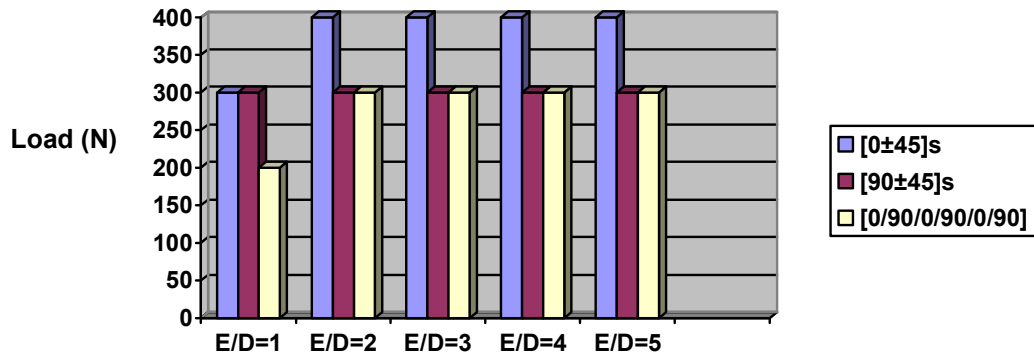


Fig 5.11 First Failure Load For [0±45]s,[90±45]s,[0/90/0/90/0/90] Lay-Ups

Similarly the values of final failure or ultimate load are obtained and shown in table and it is found that [0±45]s laminate has higher strength than [90±45]s or [0/90/0/90/0/90] lay-up.

Table 5.7 Final failure loads

Layup	Final Failure Load				
	E/D=1	E/D=2	E/D=3	E/D=4	E/D=5
[0±45]s	3100	3700	4900	4900	5100
[90±45]s	2900	3500	4700	4700	4900
[0/90/0/90/0/90]	3100	3500	4400	4400	4500

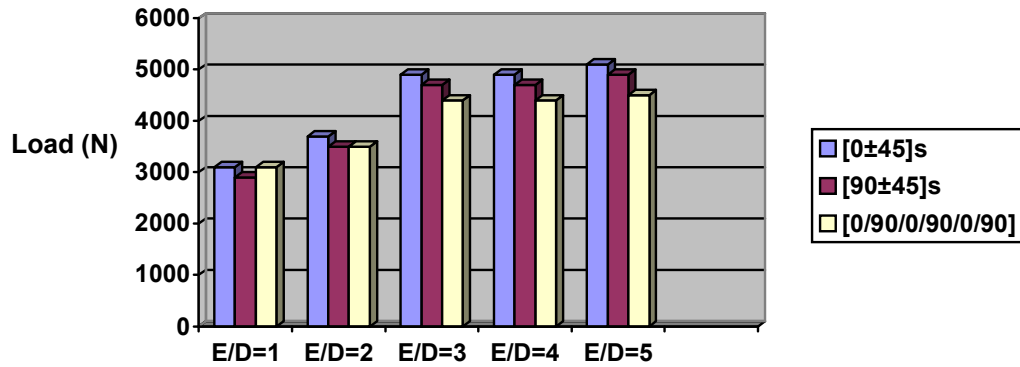


Fig 5.12 Final Failure Load For [0±45]s,[90±45]s,[0/90/0/90/0/90] Lay-Ups

5.6 DISCUSSIONS:

1. In these investigations, Hoffman and Hashin Failure criteria are used for prediction of the failure behavior. It has been seen that their results are similar.
2. Damage initiates at about 45° with respect to the loading direction and propagates through the corner side of the laminate
3. The ultimate strength values are highly dependent on the E/D ratio. The plate is weakest for E/D=1. As this ratio increases the ultimate failure load increases.
4. Ultimate strength values are sensitive to W/D and E/D values. Increasing the end distance increases the strength of the joint until a critical end distance was reached. The end distance beyond that value did not result in a significant increase in the strength of the joint. Also ultimate strength decreases with decreasing W/D ratio.

5. There is a definite dependence of ultimate as well as first failure strength on stacking sequence and joint geometry. The lay-up $[0/\pm 45]_s$ laminate was found to have higher ultimate strength than the lay-up $[90/\pm 45]_s$ laminate and $[0/90/0/90/0/90]$ laminate.

CHAPTER 6

CONCLUSION AND FUTURE SCOPE

6.1 CONCLUSION

A two dimensional progressive damage model is developed in order to predict the ultimate strength pinned composite joints under in-plane tensile loading (no bending moments). The model involves stress analysis, failure analysis and material property degradation. Failure analysis and material property degradation were implemented using a set of stress based Hashin failure criteria and Hoffman Failure Criteria and a set of appropriate degradation rules.

For the case of progressive loading, the analysis showed that after a certain load value damage initiates near the stress concentration of the hole and propagates at 45° with respect to the loading direction towards the specimen edge. The load value where damage has reached the outer specimen edge was selected for a final failure criterion. The results show that the geometry of the specimen configuration can dramatically influence initiation of damage.

It is also observed that by changing the value for 'E/D' and 'W/D' there was considerable changes in ultimate failure load for the joint. So before selecting a composite material structure/joint proper values for 'E/D' and 'W/D' must be chosen as per the structure requirement.

6.2 SCOPE FOR FUTURE WORK

The present work involves the study of damage analysis for statically loaded joints for various lamination schemes in multilayered composite laminates. The analysis was done considering laminate as a 2D element.

In the field of bolted joints in composite laminates further investigations may be carried out for the following:

1. Analysis can be extended for other type of joint structures.
2. The study can be extended for dynamic analysis.

-
1. **Fu-Kuo Chang, Kuo-Yen Chang**, "A Progressive Damage Model for Laminated Composite Containing Stress Concentrations". *Journal Of Composite Materials*, 21(1987) 834-855.
 2. **H. J. Lin & C. C. Tsai**, "Failure Analysis Of Bolted Connections Of Composites With Drilled And Moulded-In Hole", *Composite Structures*, 30 (1995) 159-168.
 3. **Nahla K. Hassan, Mohamed A. Mohamdien and Sami H. Rizkalla**, "Finite Element analysis of Bolted Connections for PFRP Composites", *Composite part B*, 27B (1996) 339-349.
 4. **Y. Xiong and O.K. Bedair**, " Analytical and Finite Element Modeling of Riveted Lap Joints in Aircraft Structure", 39th AIAA/ ASME/ ASCE/ AHS/ ASC Structures, *Structural Dynamics And Material Conference*, April 1998/ Long Beach, CA
 5. **P.P. Camanho and F.L. Matthews**, "A Progressive Damage Model for Mechanically Fastened Joints in Composite Laminates", *Journal Of Composite Materials*, 33(24) (1999) 2248-2279.
 6. **Alaattln Aktas,Ramazan Karakuzu**, "Failure Analysis Of Two- Dimensional Carbon-Epoxy Composite Plate Pinned Joint ",*Mechanics Of Composite Materials And Structures*, 6 (1999) 347–361

7. **Th. Kermanidis, G. Lebeas, K.I.Tserpes and Sp. Pentelakis**, "Finite Element Modeling Of Damage Accumulation In Bolted Composite Joints Under Incremental Tensile Loading", *ECCOMAS 2000 Barcelona*, September, (2000) ,1-14.
8. **Marie-Laure Dano, Guy Gendron and Andre Picard**," Stress And Failure Analysis Of Mechanically Fastened Joints In Composite Laminates", *Composite Structures*, 50 (2000) 287-296
9. **Q.M. Li, R.A.W. Mines, R.S. Birch**, "Static and Dynamic Behavior of Composite Riveted Joints In Tension", *International Journal Of Mechanical Sciences*, 43 (2001) 1591-1610.
10. **Okenwa I. Okoli and Ainullotfi Abdul-Latif**, "Failure in Composite Laminates: Overview of an Attempt at prediction",ELSEVIER, *Composites: Part-A: Applied Sciences and Manufacturing* , 33 (2002) 315-321.
11. **K.I. Tserpes, G. Labeas, P. Papanikos and Th. Kermanidis**, "Strength Prediction Of Bolted Joints In Graphite/Epoxy Composite Laminates", *Composites: Part B*, 33 (2002) 521–529.
12. **Bulent Murat Icten and Ramazan Karakuzu**," Progressive Failure Analysis of Pin-Loaded Carbon–Epoxy Woven Composite Plates", *Composites Science and Technology*, 62 (2002) 1259–1271.

13. **Buket Okutan and Ramazan Karakuzu**, “The Strength Of Pinned Joints In Laminated Composites”, *Composites Science and Technology*, 63 (2003) 893–905.
14. **B. Yang , E. Pan , F.G. Yuan**. “Three-Dimensional Stress Analyses In Composite Laminates With A Pinned Hole”, *International Journal Of Solids And Structures*, 40 (2003) 2017–2035.
15. **J. Wang,P.J. Callus, M.K. Bannister**,” Experimental And Numerical Investigation Of The Tension And Compression Strength Of Un-Notched And Notched Quasi-Isotropic Laminates”, *Composite Structures*, 64 (2004) 297–306.
16. **E.J. Barbero,G.F. Abdelal,A. Caceres**, “A Micromechanics Approach For Damage Modeling Of Polymer Matrix Composites” ,*Composite Structures*, 67 (2005) 427–436.
17. **C.T. McCarthy, M.A. McCarthy, V.P. Lawlor**, “Progressive Damage Analysis Of Multi-Bolt Composite Joints With Variable Bolt–Hole Clearances”, *Composites: Part B*. 36 (2005) 290–305
18. **Ramazan Karakuzu,Tayfun Gulem, Bulent Murat Icten**,” Failure Analysis Of Woven Laminated Glass–Vinylester Composites With Pin-Loaded Hole”, *Composites Science and Technology*, 72 (2006) 27–32
19. **Tirupathi R. Chandrupatla and Ashok D. Belegundu**, “Introduction to Finite Elements in Engineering “,Third Edition.

20. **Autar K.Kaw**, "Mechanics of Composites Materials", *CRC Press Boca Raton*, New York, 1997